EXTENDING THE THEORY FOR THE PRIMARY CONSOLIDATION OF SOILS

EXTENDING THE THEORY FOR THE PRIMARY CONSOLIDATION OF SOILS

By

CHIH TSUNG HWANG, B.Sc.

A Thesis

Submitted to the Faculty of Graduate Studies

in Partial Fulfilment of the Requirements

for the Degree

Master of Engineering

McMaster University

September 1966

MASTER OF ENGINEERING (1966) McMASTER UNIVERSITY
(Civil Engineering) Hamilton, Ontario

TITLE: Extending the Theory for the Primary Consolidation of Soils

AUTHOR: Chih Tsung Hwang, B.Sc. (National Taiwan University)

SUPERVISOR: Professor Nyal E. Wilson

NUMBER OF PAGES: vii, 100

SCOPE AND CONTENTS: The classical Terzaghi Theory was extended by accounting for the variations of permeability during consolidation. With the aid of X-ray techniques, investigations on the significance of the variation of permeability, as well as the variations of void ratio and effective pressure, were conducted. Effects of the conventional consolidometer boundary on consolidation testing were studied.

ACKNOWLEDGEMENTS

I wish to express my sincere gratitude to Professor Nyal E. Wilson for his help and encouragement during the course of this work, which was supported by the Defence Research Board of Canada, Grant Number 9768-04 and National Research Council of Canada, Grant Number A1058.

I am grateful to Dr. M. K. Ho and Dr. W. K. Tso for their advice and assistance in the analysis.

Technical assistance by Mr. Jim Bryson to the experimental work is gratefully acknowledged.

TABLE OF CONTENTS

LIST OF FIGURES

LIST OF TABLES

CHAPTER 1

INTRODUCTION

The progressive settlement of structural foundations on compressible soils, such as clay and peat, raises problems of practical importance in construction. The theory of consolidation of soil, derived by Terzaghi (1925) and based on simplifying assumptions, has been applied to the field as a practical instrument for analyzing the settlement problems.

The discrepancies between the values obtained from theoretical predictions and those of field measurement have urged investigations and studies on time-dependent behavior of the soil skeleton during the process of consolidation. Some terms like "Secondary consolidation","Secondary time effect", "Secular compression", and "Secondary compression" were named to describe the soil behavior which could not be explained by Terzaghi's Theory which applied the principles of hydrodynamics and heat transfer to consolidation. Thus, consolidation has generally been divided into two phases; one is "Primary consolidation", (Terzaghi's Theory) and the other is "Secondary consolidation".

In Terzaghi's Theory, the permeability of soil during consolidation was assumed to be constant, but it has

been found that the permeability of soil decreases as the void ratio decreases. The purpose of this research work is to investigate the significance of the variation of permeability, as well as the variations of void ratio and effective pressure. The experimental testing was conducted with the aid of X-ray techniques which showed the deformations in the soil sample during consolidation. Pressure transducers were used for the measurements of pore water pressures and total pressures at the sample bottom.

By relating the effective pressure, the void ratio, and the permeability, the classical Terzaghi Theory was extended by accounting for the variations of the permeability during consolidation. This "Extended Theory" shows the effects on consolidation of various load increment ratios and the effects of various "Flow-Loading Parameters" which relate the variations between void ratio, effective pressure, and permeability. In Terzaghi's Theory, the curves of degree of consolidation and dissipation of pore water pressure are independent of load increment ratio.

CHAPTER 2

LITERATURE REVIEW

Consolidation is a time-dependent volume reduction involving a decrease of water content. Terzaghi (1925) developed the classical concepts for consolidation with a single hydrodynamic process, which was later termed "Primary consolidation". It was assumed that for every void ratio there exists a maximum effective pressure that can be supported by the intergranular soil skeleton. When an applied loading is in excess of the capacity of the soil skeleton at a particular void ratio, the excess pressure is supported by the pore water within the voids, thus excess pore water pressure is developed. The development of excess pore water causes water to dissipate from the soil according to Darcy's Law. The resulting decrease in void ratio increases the supporting capacity of the intergranular soil skeleton and thus relieves some of the excess pore water pressure. This process continues until the excess pore water pressure is reduced to zero and the applied loading is supported entirely by the soil structure. The mechanism of classical consolidation is the development and subsequent dissipation of pore water pressures.

It has been found that the behavior of cohesive soils, such as clay and peat, under one dimensional consolidation cannot be explained satisfactorily by Terzaghi's Theory. The theory implies a final compression (complete consolidation) by applying hydrodynamics to the process. Observing the settlement of embankments and structures and correlating the results of undisturbed soil sample tests, Buisman (1936) gave a formula for the secular time effect. This effect, governing the portion of the settlement after the dissipation of pore water pressure, was termed "Secondary consolidation". This time dependent behavior of the soil skeleton had not been considered in Terzaghi's Theory which attributed the settlement of soil to the expulsion of pore water from the assumed elastic soil skeleton under external loadings. The portion of the settlement during the period of pore water pressure dissipation was termed "Primary consolidation". Based on the possibility of isolating the hydrodynamic phase (primary consolidation) from the secular time phase (secondary consolidation) in the whole process of consolidation, Koppejan (1948) expressed formulae combining the Terzaghi theory and the Buisman secular time effect. The validity of these formulae depends upon the application of the Casagrande conventional method to the basic settlement--logarithmic time curves.

Leonards and Girault (1961) found that, depending upon the load increment ratio and upon whether or not the

pressure increment straddled the effective preconsolidation pressure, the conventional e-logt curves could be classified according to three typical shapes, two of which could not isolate hydrodynamic phase from secular time phase using Casagrande's method. In Terzaghi's Theory, the non-dimensional theoretical curve was independent of load increment ratio because of the assumption that the non-linear continuity equation could be linearized.

Taylor and Merchant (1942) started the investigation on the rheological properties of soil skeleton by taking into account the shearing strain rate and the effective pressure duration, and proposed a spring and linear dashpot as a model with the behavior of the soil skeleton related to the time rate of compression. Tan (1957) studied the rheological properties of clays with the help of a plastometer. Assuming the soil skeleton as a porous Maxwell body, Tan extended Biot's general theory (1941) on three-dimensional consolidation which considered the soil skeleton to be elastically reversible, porous and filled with water. Gibson and Lo (1961) used a Voigt element to describe analytically the mechanics of secondary consolidation sharing the assumption by Taylor and Merchant (1942) that the rate of secondary consolidation was proportional to the undeveloped secondary compression of the soil skeleton and the ultimate amount of secondary compression was assumed to be known. Wahls (1962) used a model that differed from those

previously proposed. The model combined, in series, a Kelvin body and a secondary dashpot to describe the mechanism of the consolidation process. The dashpot in the Kelvin body illustrated the concept of the hydrodynamic process; the secondary dashpot with a variable dashpot coefficient illustrated the concept of secondary consolidation.

It was found that all these rheological models could not explain satisfactorily the three types of consolidation curve proposed by Leonards and Girault (1961). Barden (1965) extended these linear rheological models of the Terzaghi-Taylor concept of secondary consolidation by proposing a more natural non-linear rheological model obtaining an approximate finite difference solution by means of a digital computer. The dependency of secondary consolidation on sample height and load increment ratio was presented.

A number of investigations on the consolidation of compressible soils were made. A summary of the investigations on secondary consolidation could be made as follows:

(a) An approximate linear relationship between settlement and the logarithm of time for secondary consolidation, exists for both clay and peat. (Buisman, 1936; Hanrahan, 1954)

(b) The ratio of the secondary consolidation per cycle of time, R_s, on the settlement-log time scale to the primary

consolidation, R_{100}, increased in a consistent pattern with decreasing load increment ratio, irrespective of the total pressure. (Leonards and Girault, 1961; Wahls, 1962)

(c) The coefficient of secondary consolidation, C_α, (expressed in terms of volumetric strain or void ratio change per cycle of log time) was dependent on void ratio (and, consequently, the total pressure) and was independent of the magnitude of the pressure increment and the pressure increment ratio. (Wahls, 1962)

(d) The coefficient of secondary consolidation, C_α, was considerably affected by temperature, therefore, C_α for thin samples in laboratory testing was not necessarily valid for thick layers in the field. (Leonards and Ramiah, 1959; Lo, 1961)

(e) The influence of the length of drainage on the rate of secondary consolidation has been proposed in three hypotheses: (1) The rate of secondary consolidation was independent of the length of drainage. (Lake, 1961; Simons, 1961; Brawner, 1961) (2) The rate of secondary consolidation was proportional to the length of drainage. (Thompson and Palmer, 1951; Kapp, 1951) (3) The rate of secondary consolidation was proportional to the square of the length of drainage. (Hanrahan, 1954; Lea and Brawnen, 1959)

(f) A hypothesis was proposed that the mechanism of secondary consolidation was a viscous or plastic flow of the soil skeleton. (Taylor, 1942; Tan, 1957; Schroeder and

Wilson, 1962)

Recent investigations on primary consolidation have been conducted. The Terzaghi theory, simplifying the relationship of the variations in void ratio, permeability, and effective pressures, was unable to explain the primary consolidation satisfactorily. McNabb (1960) derived the one dimensional consolidation equation in a very general form. Schiffman (1958), by some exponential approximation, took into account the varying permeability and time-dependent loading for the consolidation theory. Davis and Raymond (1965) derived a non-linear theory of one-dimensional consolidation for the boundary conditions of the oedometer.

As primary and secondary consolidation are parts of a single continuous process, the relationship between the characteristics of primary consolidation and secondary time effect are controversial. Hansen (1961) suggested an approximate model law for simultaneous primary and secondary consolidation with the assumption that secondary consolidation started as soon as an increase in effective pressure was developed. The validity of this approximation was limited because of the assumption that the settlements observed in consolidation testing could represent the actual properties of the undistrubed soil.

Abbott (1960) developed a numerical method to deal with the consolidation problems of non-homogeneous soils. The results, after comparing the calculated and prototype

settlements, indicated that the variations of permeability and compressibility required critical investigation.

For highly compressible soils like peat, the change of permeability corresponding to the change of void ratio and the effective pressure is known. It is important to have an understanding of the mechanism of primary consolidation which affects inherently the secondary consolidation and thus the whole process of consolidation. This is the purpose of this thesis.

CHAPTER 3

EXTENDED THEORY ON ONE DIMENSIONAL PRIMARY CONSOLIDATION OF SOIL

To derive an equation representing the mechanism of the one-dimensional consolidation of soil, the following assumptions have been made:

Assumptions

(1) The soil skeleton is initially isotropic, homogeneous and is fully saturated with water. Both the water and the solid constituents of the soil skeleton are incompressible; therefore the change in the volume of the soil skeleton is equal to the volume of the pore water expelled.

(2) Fluid flow and the movement of soil particles are assumed to be along the vertical axis. Darcy's law is valid.

(3) The relationship between the void ratio and effective pressure is

$$e = e_o - a \log \frac{P'}{P'_o}$$

Where e_o and e are the void ratios corresponding to the effective pressures P'_o at time t=o, and P'_1 at time t=t respectively. (The viscous characteristics of the soil

skeleton under constant effective pressure have not been taken into account here.) a is compression index.

(4) To consider the variation of the permeability k, corresponding to the change of void ratio and effective pressure during the process of consolidation, the following relationship is assumed:

$$\frac{k}{1+e}(P')^n = \frac{k_o}{1+e_o}(P_o')^n$$

where k and k_o are the permeabilities corresponding to e and e_o respectively.

or

$$\log\left(\frac{k}{1+e} \Big/ \frac{k_o}{1+e_o}\right) = -n \log (P'/P_o')$$

where n=tan θ which is the magnitude of the rate of change of $\log\left(\frac{k}{1+e}/\frac{k_o}{1+e_o}\right)$ with respect to $\log (P'/P_o)$. The angle θ between the characteristic line and the abscissa, as shown in Fig. 1, could be considered a parameter representing the soil property.

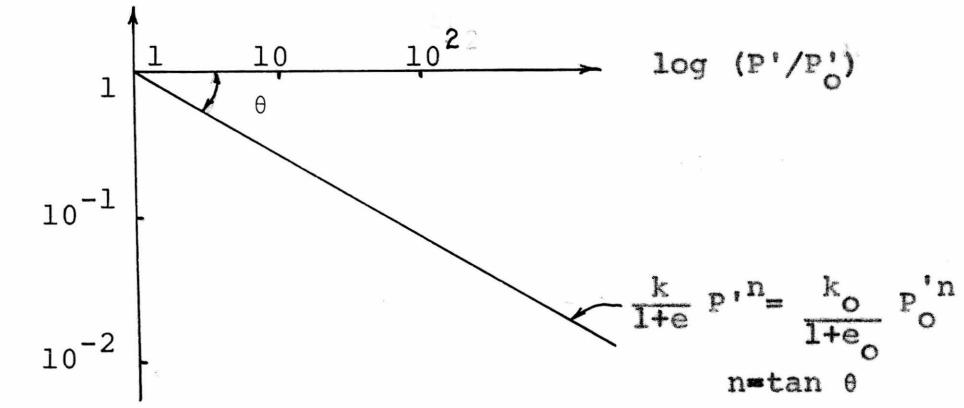

Fig. 1

Let $\frac{k}{1+e} P'^{n} = K$

where $K = \frac{k_o}{1+e_o} P_o'^{n}$ = Initial soil condition.

(5) The total pressure is the sum of the effective pressure and the excess pore water pressure. The total pressures at a horizontal plane are uniform; so is the effective stress. Therefore, the settlement of soil particles in this horizontal layer will be the same.

Derivation

Fig. 2 is a sketch describing a soil stratum under consolidation beneath a footing. The footing has a unit area on which a total pressure, P, is applied.

Consider a soil element ABCD of unit horizontal area. Let the thickness of the solid particles be dz. If its void ratio is e, the volume of the void in this element will be edz. Defining the distance between AD and BC of the soil element as

$$dL = dz + edz = (1+e)dz$$

the distance, at time t, from the top of the soil stratum to a layer at depth z of the solid particles will be

$$L(z,t) = \int_o^z \left[1+e(z,t) \right] dz$$

Let v be the vertical velocity of water flow at the plane AA'D'D, and let V be the volume of the soil element. The change of the volume per unit time per unit area will be the difference of the flow velocity through the soil element, that is,

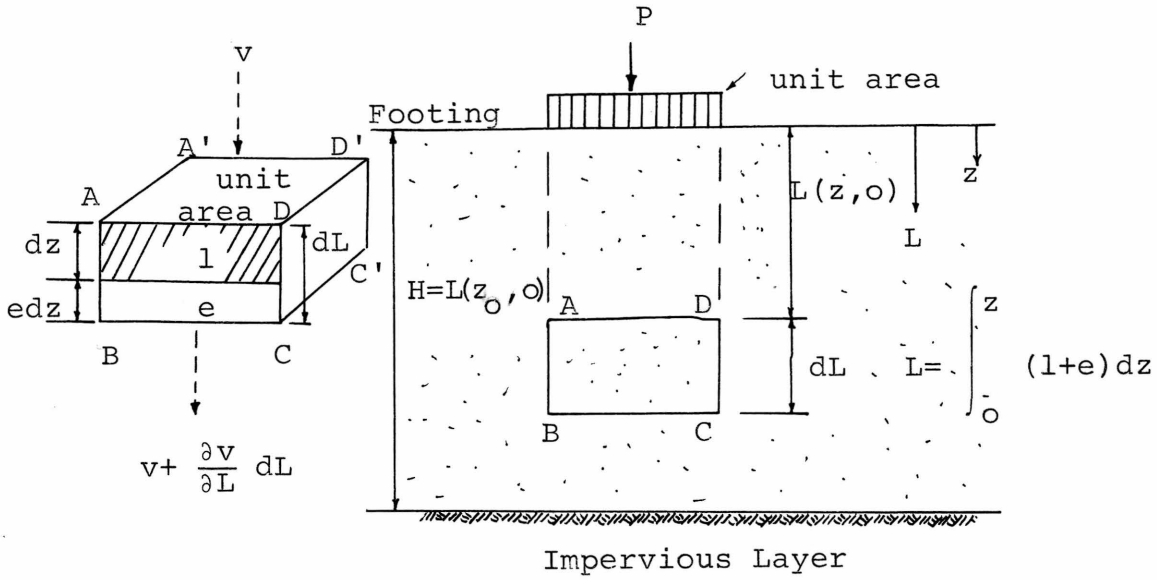

Fig. 2

$$\frac{\partial V}{\partial t} = -(v + \frac{\partial v}{\partial L} dL) + v = -\frac{\partial v}{\partial L} dL = -\frac{\partial v}{\partial z} dz$$

since

$$V = dL = (1+e)dz$$

therefore

$$\frac{\partial V}{\partial t} = \frac{\partial}{\partial t} \left[(1+e)dz \right] = \frac{\partial e}{\partial t} dz.$$

According to Darcy's law,

$$v = -ki = -k \frac{\partial h}{\partial L}$$

where h is the pressure head, and $\frac{\partial h}{\partial L} = i$.

Let u(z,t) be the excess pore water pressure at that layer

then $$h = \frac{u(z,t)}{\gamma w}$$

where γ_w = unit weight of water.

Now, $$v = -k \frac{\partial h}{\partial L} = -k \frac{\partial}{\partial L} \left[\frac{u(z,t)}{\gamma w} \right]$$

$$= \frac{-k}{\gamma w (1+e)} \cdot \frac{\partial u(z,t)}{\partial z}$$

Therefore,

$$\frac{\partial e}{\partial t}\,dz = \frac{\partial}{\partial z}\left[\frac{k}{(1+e)\gamma w}\,\frac{\partial u}{\partial z}\right]dz.$$

The equation of continuity will be

$$\frac{\partial e(z,t)}{\partial t} = \frac{\partial}{\partial z}\left\{\frac{k(z,t)}{[1+e(z,t)]\gamma w}\,\frac{\partial u(z,t)}{\partial z}\right\} \qquad (1)$$

This equation was derived by McNabb (1960).

Since

$$P = P'(z,t) + u(z,t)$$

$$\frac{\partial u(z,t)}{\partial z} = -\frac{\partial P'(z,t)}{\partial z}$$

$$e = e_o - a \log (P'/P'_o)$$

$$\frac{\partial e}{\partial t} = -a'\,\frac{1}{P'}\,\frac{\partial P'}{\partial t}$$

where

$$a' = \frac{a}{\log_e 10}$$

Let

$$\frac{k}{1+e}\,(P')^n = K$$

where

$$K = \frac{k_o}{1+e_o}\,(P'_o)^n \text{ ——— Initial condition.}$$

Substituting into Eq. (1)

$$\frac{a'}{P'(z,t)}\,\frac{\partial P'(z,t)}{\partial t} = \frac{K}{\gamma w}\,\frac{\partial}{\partial z}\left\{\frac{1}{P'(z,t)^{\,n}}\,\frac{\partial P'(z,t)}{\partial z}\right\}$$

or

$$\frac{1}{P'(z,t)}\,\frac{\partial P'(z,t)}{\partial t} = K'\,\frac{\partial}{\partial z}\left\{\frac{1}{P'(z,t)^{\,n}}\,\frac{\partial P'(z,t)}{\partial z}\right\}$$

where

$$K' = \frac{K}{a'\gamma w} \qquad (2)$$

Since

$$L(z,t) = \int_o^z \left[1 + e(z,t) \right] dz$$

$$L(z,o) = \int_o^z \left[1 + e(z,o) \right] dz$$

$$dL(z,o) = (1+e_o)dz$$

$e_o = e(z,o)$ = Initial void ratio.

Substituting into Eq. (2)

$$\frac{1}{P'(L,t)} \frac{\partial P'(L,t)}{\partial t} = \frac{k_o(1+e_o)(P'_o)^n}{a' \gamma w} \frac{\partial}{\partial L} \left\{ \frac{1}{P'(L,t)^n} \frac{\partial P'(L,t)}{\partial L} \right\}$$

where

$$L = L(z,o). \qquad (3)$$

Eq. (3) is the general equation governing the one-dimensional primary consolidation of soil. The initial and boundary conditions are:

i)	$P'=P'_o$	for $o < L < H$	$t=o$;
ii)	$P'=P'_o + \Delta P'_o=P'_1$	for $o < L < H$	$t\to\infty$;
iii)	$P'=P'_o + \Delta P'_o=P'_1$	for $L=o$	$t>o$;
iv)	$\frac{\partial P'}{\partial L} = o$	for $L=H$	$o \leq t \leq \infty$,

where $\Delta P'_o$ is the load increment, therefore, Δ will be the load increment ratio.

Eq. (3) can be rewritten into the well known Terzaghi form,

$$\frac{\partial P'(L,t)}{\partial t} = C_v \frac{\partial^2 P'(L,t)}{\partial L^2}$$

by making the following simplifications:

a) $n=o$

b) $\frac{de}{dp'} = -a_v$ instead of assumption (3)

$$\frac{de}{dp} = -\frac{a'}{p'}$$

where a_v was defined by Terzaghi as the coefficient of compressibility, and C_v is called the coefficient of consolidation which equals $\frac{k(1+e)}{a_v \gamma w}$. Such kind of simplification neglecting the variation among the void ratio, permeability, and effective pressure made the Terzaghi consolidation equation be independent of load increment ratio.

If n is defined as 1, that is, the Flow-Loading Parameter θ, representing the soil property, is 45^o, Eq.(3) becomes

$$\frac{1}{P'(L,t)} \frac{\partial P'(L,t)}{\partial t} = \frac{k_o(1+e_o)P'_o}{a'\gamma w} \frac{\partial}{\partial L}\left\{ \frac{1}{P'(L,t)} \frac{\partial P'(L,t)}{\partial L} \right\}$$

This is the form derived by Davis and Raymond (1965) by different approach with some simplifications.

Solutions of the extended equation

The extended equation governing the physical property of one dimensional consolidation of soil is

$$\frac{1}{P'(L,t)} \frac{\partial P'(L,t)}{\partial t} = \frac{k_o(1+e_o)(P'_o)^n}{a' \gamma w} \frac{\partial}{\partial L}\left\{ \frac{1}{(P'(L,t))^n} \frac{\partial P'(L,t)}{\partial L} \right\}$$

or

$$\frac{1}{P'(L,t)} \frac{\partial P'(L,t)}{\partial t} = C_v' \frac{\partial}{\partial L} \left\{ \frac{(P_o')^{n-1}}{[P'(L,t)]^n} \frac{\partial P'(L,t)}{\partial L} \right\} \qquad (4)$$

where $C_v' = \frac{k_o(1+e_o)P_o'}{a' \gamma_w}$ = coefficient of consolidation.

Let $\chi = \frac{L}{H} = \frac{L(z,o)}{L(z_o,o)}$ = the depth ratio of any horizontal plane at time t=o to the initial depth of the soil stratum H, which is $L(z_o,o)$; z_o is the total thickness of the solid particles of the soil stratum.

$p = \frac{P'}{P_o'}$, the ratio of effective pressure P' to the preconsolidated pressure P_o'.

$T = \frac{C_v' t}{H^2}$, the time factor. χ, p, T are dimensionless.

Substituting, Eq. (4) becomes the non-dimensional form:

$$\frac{1}{p(\chi,T)} \frac{\partial p(\chi,T)}{\partial T} = \frac{\partial}{\partial \chi} \left[\frac{1}{p^n(\chi,T)} \frac{\partial p(\chi,T)}{\partial \chi} \right] \qquad (5)$$

with the following initial and boundary conditions:

i) $p=1$ for $o < \chi < 1$, $T=o$;

ii) $p = \frac{P_o'+\Delta P_o}{P_o'} = 1+\Delta$ for $\chi < \chi < 1$, $T=\infty$;

Δ is load increment ratio

iii) $p=1+\Delta$ for $\chi=o$ $T>o$;

iv) $\frac{\partial p}{\partial \chi} = o$ for $\chi=1$ $o \leq T \leq \infty$.

1) For $n \neq 1$,

let $C(\chi,T) = p(\chi,T)^{(1-n)}$ or $p(\chi,T) = C(\chi,T)^{\frac{1}{1-n}}$.

Eq. (5) becomes

$$\frac{1}{C(\chi,T)} \frac{\partial C(\chi,T)}{\partial T} = \frac{\partial^2 C(\chi,T)}{\partial \chi 2} \qquad (6)$$

This non-linear partial differential equation was solved by numerical analysis with the help of digital computer.

Let C(i,j) be the value of C at depth ratio χ=i, time factor T=j.

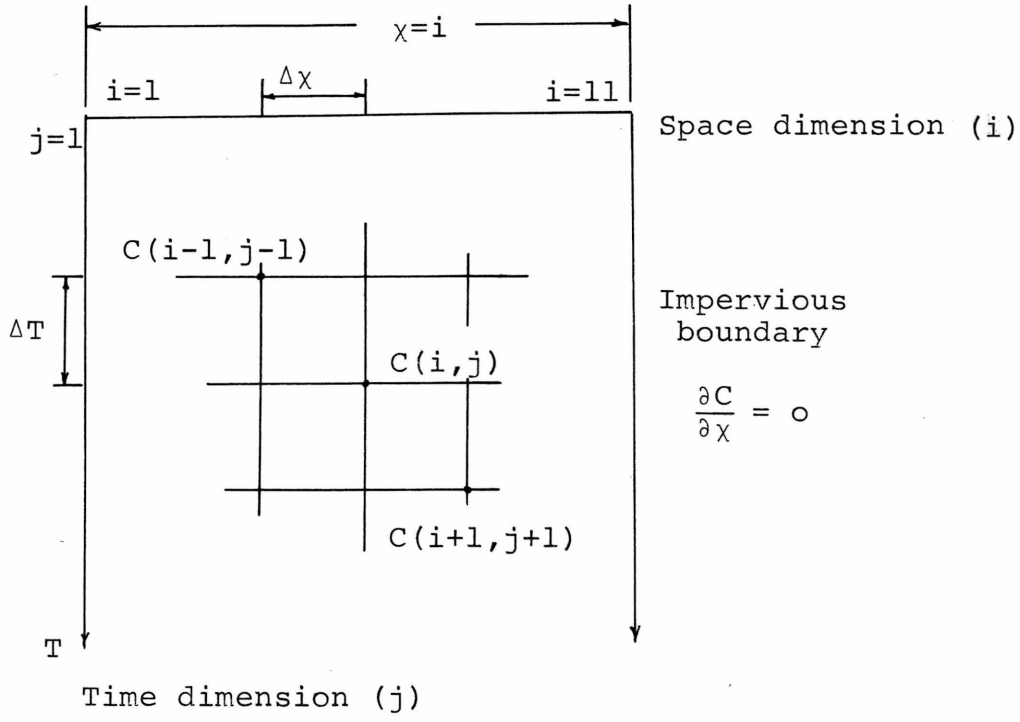

Fig. 3 Finite Difference Space-Time Grid

Eq. (6) becomes

$$\frac{1}{C(i,j)} \frac{C(i,j+1)-C(i,j)}{\Delta T} = \frac{1}{\Delta\chi^2} \left\{ C(i+1,j)+C(i-1,j)-2C(i,j) \right\}$$

or

$$\frac{1}{2} \frac{C(i,j+1)-C(i,j-1)}{C(i,j) \quad \Delta T} = \frac{1}{\Delta\chi^2} \left\{ C(i+1,j)+C(i-1,j)-2C(i,j) \right\}$$

Let

$$\Delta\chi = 0.1 \qquad R = \frac{\Delta T}{\Delta\chi^2} = \frac{\Delta T}{0.01}$$

$\therefore \Delta T = R \times 0.01$

where R is the increment ratio in the matrix representing the depth ratio and time factor. In order to avoid oscilatory effect, proper values of R for different boundary conditions were found, and were shown in appendix B.

Degree of consolidation (S) is

$$S = \frac{\int_o^1 (e_o - e) d\chi}{\int_o^1 (e_o - e_f) d\chi} \quad ;$$

where e_f is the final void ratio for a given load increment.

$$S = \frac{\sum_1^{10} \log \frac{P'}{P'_o} \Delta\chi}{\sum_1^{10} \log \frac{P'_o + P'_o}{P'_o} \Delta\chi} = \frac{\sum_1^{10} \log p \ \Delta\chi}{\sum_1^{10} \log (1+\Delta) \ \Delta\chi}$$

$$= \frac{\sum_1^{10} \log C(i,j)^{\frac{1}{1-n}} \ x0.1}{\sum_1^{10} \log (1+\Delta) \ x0.1} = \frac{\sum_1^{10} \log C(i,j)^{\frac{1}{1-n}}}{10 \times \log (1+\Delta)}$$

Let U(i,j) be the pore water pressure ratio, that is, the ratio of pore water pressure at any depth ratio χ and time factor T to the theoretical maximum pore water pressure $\Delta P'_o$,

$$U(i,j) = \frac{P'_o+\Delta P'_o - P'(i,j)}{\Delta P'_o} = \frac{1+\Delta - p(i,j)}{\Delta}$$

$$= \frac{1+\Delta - C(i,j)^{\frac{1}{1-n}}}{\Delta}$$

Fixing the given boundary conditions on the finite difference space-time grid (Fig. 3), Eq. (6) was solved with the simple explicit process. The curves of degree of consolidation (S) and dissipation of maximum pore water pressure (U) versus time factor (T) were plotted in Fig. 14 and Fig. 15.

2) For n = 1,

Eq. (5) becomes

$$\frac{1}{p(\chi,T)} \frac{\partial p_1(\chi,T)}{\partial T} = \frac{\partial}{\partial \chi}\left\{\frac{1}{p_1(\chi,T)} \frac{\partial p_1(\chi,T)}{\partial \chi}\right\}$$

or

$$\frac{\partial}{\partial T} \log p_1(\chi,T) = \frac{\partial^2}{\partial \chi^2} \log p_1(\chi,T)$$

where

$$p_1 = \frac{P'}{P'_f} = \frac{P'}{P'_o+\Delta P'_o} = \frac{P'}{P'_o} \frac{1}{1+\Delta} = \frac{p}{1+\Delta}$$

$P'_f = P'_o+\Delta P'_o$ = final effective pressure.

The initial and boundary conditions become

i) $p_1 = \frac{1}{1+\Delta}$ $\quad o < \chi < 1 \quad$ $T = o$

ii) $p_1 = 1$ $\quad o < \chi < 1 \quad$ $T = \infty$

iii) $p_1 = 1$ $\quad \chi = o \quad$ $T > o$

iv) $\frac{\partial p_1}{\partial \chi} = o$ $\quad \chi = 1 \quad$ $o \leq T \leq \infty$

This is the same form as Terzaghi's theory, and is the same as Davis and Raymond's equation, therefore,

$$\log p_1 = \left(\log \frac{1}{1+\Delta} \right) \sum_{N=o}^{N=\infty} \frac{2}{M} (\text{Sin } M\chi)\, e^{-M^2 T}$$

or

$$p_1 = \left(\frac{1}{1+\Delta} \right)^B$$

where

$$B = \sum_{N=o}^{N=\infty} \frac{2}{M} (\text{Sin } M\chi)\, e^{-M^2 T}$$

$$M = (2N+1)\, \pi/2$$

$$T = \frac{C_v' t}{H^2} = \text{time factor}$$

$$\chi = \frac{L(z,o)}{H} = \text{depth ratio at the original position.}$$

The pore water pressure ratio

$$U(\chi,T) = \frac{P_o' + \Delta P_o' - P'}{\Delta P_o'} = \frac{1+\Delta-p}{\Delta} = \frac{1+\Delta - (1+\Delta)p_1}{\Delta}$$

$$U(\chi,T) = \frac{1+\Delta}{\Delta} (1-p_1) = \frac{1+\Delta}{\Delta} \left\{ 1 - \left(\frac{1}{1+\Delta} \right)^B \right\}$$

Degree of consolidation

$$S = \frac{\int_0^1 (e_o - e)\, d\chi}{\int_0^1 (e_o - e_f)\, d\chi}$$

$$S(\chi,T) = \frac{\int_0^1 \log \frac{P'(\chi,T)}{P'_o}\, d\chi}{\int_0^1 \log \frac{P'_f}{P'_o}\, d\chi}$$

$$= \frac{\int_0^1 \log \frac{P'}{P'_f} \cdot \frac{P'_f}{P'_o}\, d\chi}{\int_0^1 \log \frac{P'_f}{P'_o}\, d\chi} = 1 + \int_0^1 \frac{\log p_1}{\log \frac{P'_f}{P'_o}}\, d\chi$$

$$= 1 - \int_0^1 \log p_1 \Big/ \log \frac{1}{1+\Delta}\, d\chi = 1 - \int_0^1 B\, d\chi$$

$U(\chi,T)$ and $S(\chi,T)$ were calculated with computer.

The curves of degree of consolidation and dissipation of pore water pressure are shown in Fig. 14 and Fig. 15. Discussions on this extended theory are presented in Chapter 6.

CHAPTER 4

EXPERIMENTAL APPARATUS AND PROCEDURE

Experimental Apparatus

A consolidometer was used to determine the rate of deformation within the sample and to measure the pore water pressures along the consolidometer wall. X-rays were used to record the deformation within different zones of the sample; the X-ray pictures showed the movements of markers placed in the sample. The consolidometer was kept at constant temperature for each test using a 4 cu. ft. water bath. The water temperature was kept constant by a thermoregulator and a mixer. Fig. 4 shows the apparatus.

A) Consolidometer -- The consolidometer which was designed to determine the characteristics of one-dimensional consolidation, consisted of an aluminium cylinder, base and cover, and loading piston. Fig. 5 shows the consolidometer.

The aluminium cylinder was lined with teflon to minimize the friction between the soil sample and the cylinder wall, and the friction between the piston and the wall. The teflon liner was 1/2" thick, 4-1/32" I.D., and 12-1/8" high. Two openings, 1-3/4" wide and 5-1/4" long

FIG. 4 EXPERIMENTAL APPARATUS

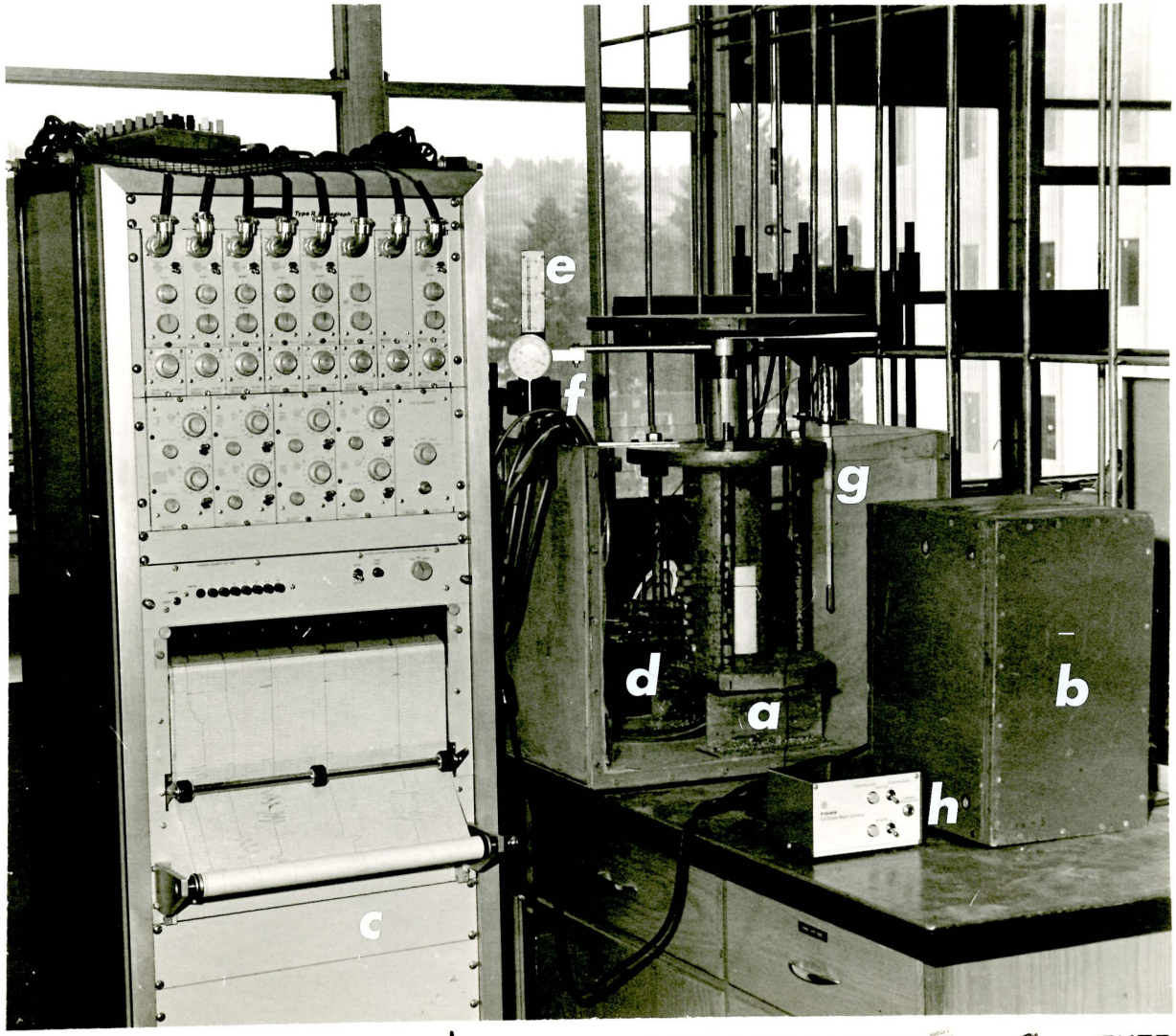

a — CONSOLIDOMETER

b — X RAY APPARATUS

c — RECORDER

d — PORE PRES. TRANSDUCERS

e — DIAL GAUGE

f — MIXER

g — THERMOREGULATER

h — FISHER UNITIZED BATH CONTROL

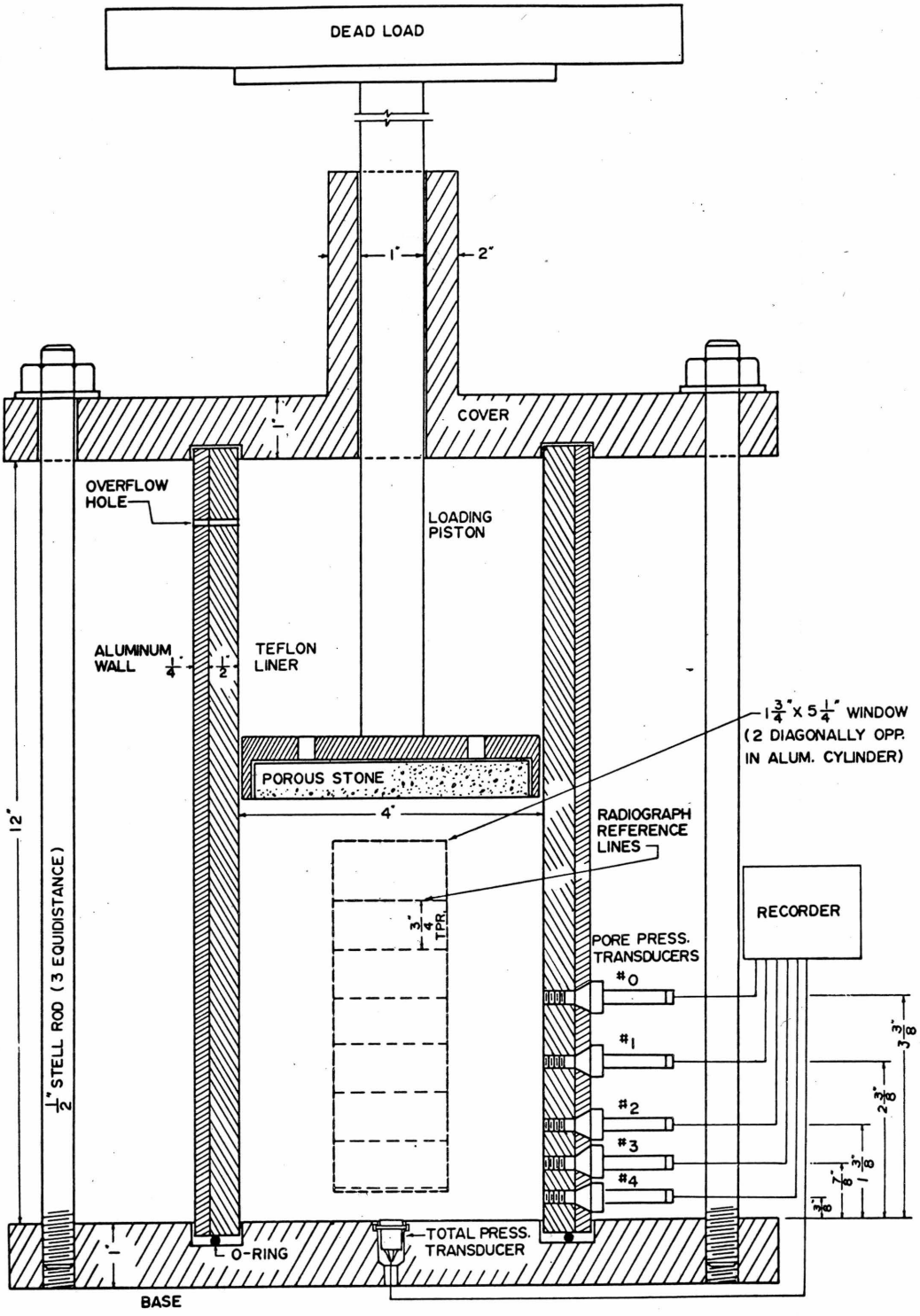

FIG. 5 CONSOLIDOMETER

were cut in the aluminium wall diametrically opposite to each other. In one opening, reference lines were placed to relate the movement of soil to the consolidometer; these reference lines, consisting of 0.015" lead solder, showed on X-ray pictures. On one side, 90^{o} from the openings, five transducers for pore water pressure measurements were fixed to the cylinder; the transducers were enclosed in brass casings to waterproof the connection. The distances of these casings from the bottom of the cylinder were 3/8", 7/8", 1-3/8", 2-3/8", 3-3/8". To measure the total pressure at the bottom of the sample, a transducer was located at the center of the surface of the base which acted as the bottom of the cylinder. The cylinder was tightened to the cover and the base by three 1/2" screwed rods. An O-ring sealed the cylinder to the base. The soil sample was loaded by means of a piston and dead weights.

B) Transducers and Casings -- Pressure transducers were used for pore-water pressure and total pressure measurements. A displacement of the diaphragm of the transducer occurs when a pressure is applied; the displacement changes the length of four strain gauges connected to the diaphragm and wired in the form of a Wheatstone Bridge. Any changes in the lengths and consequently in the resistances of these gauges alter the electrical balance of the

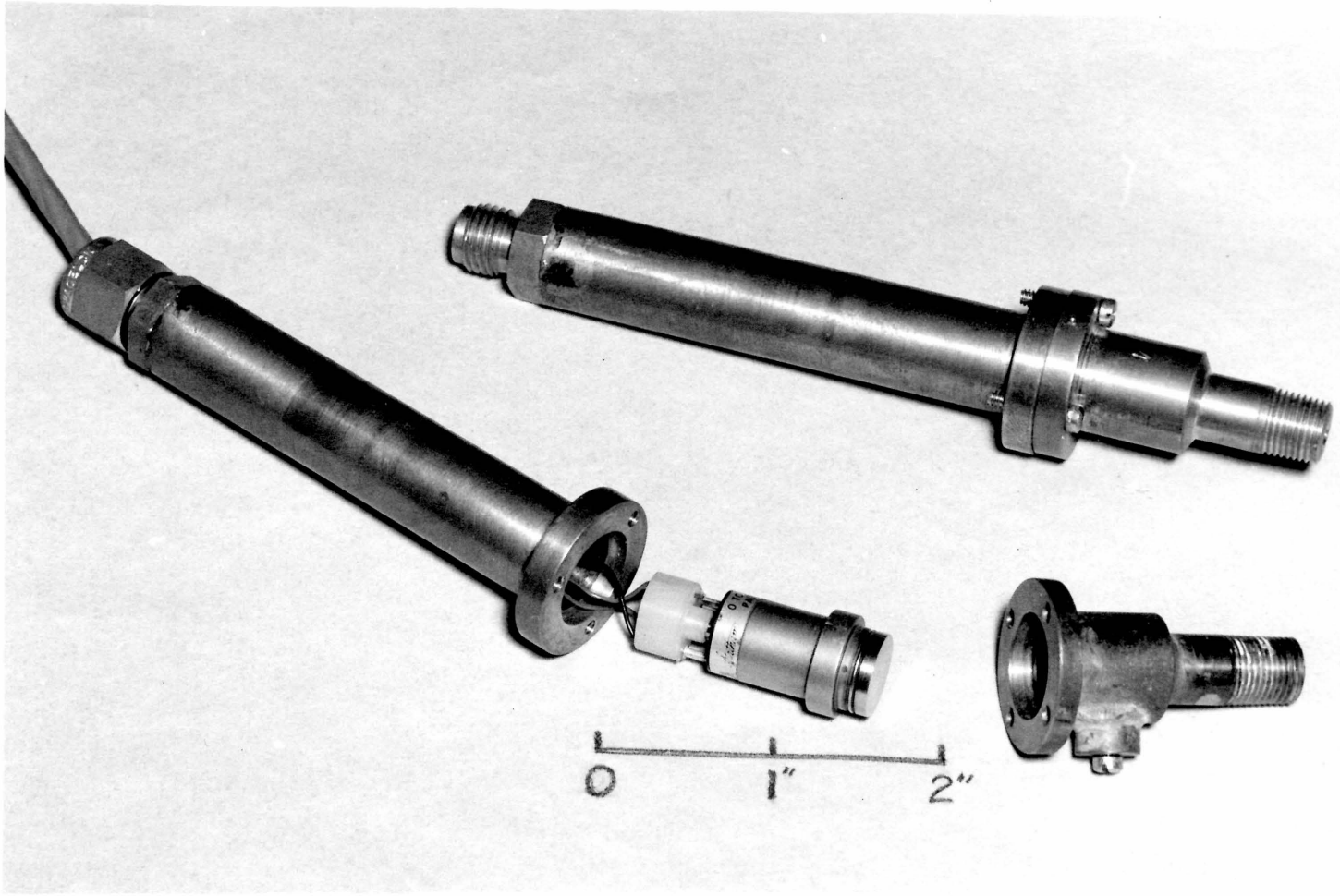

FIG. 6 TRANSDUCER AND HOUSING

bridge. These changes can be calibrated against applied pressure. Fig. 6 shows the transducer and the casing.

The model number of the transducers is PA-208-TC-25-350 from Statham Instruments Inc., Los Angeles. The following data are quoted from the company's publication for one of the transducers used.

a) Serial No.: 34730

b) Pressure Range: O to 25 Psi (with 100% overload)

c) Excitation: 7 Volts (A.C. or D.C.)

d) Input Resistance: 346 Ohms

e) Output Resistance: 346 Ohms

f) Compensated Temperature Interval: -65F to +250F

g) Volume Change at the diaphragm at full scale pressure: approximately 0.2×10^{-6} in^3

h) Calibration Factor: 402.2 Microvolts (open circuit) per volt per Psi

All the outputs from the transducer were connected to a Beckman multi-channel recorder. (Fig.4) The recorder was the Beckman-Offner Type R Dynograph from Beckman Instruments, Inc., Offner Division, Schiller Park, Illinois. Its basic modules were couplers, preamplifiers, power amplifiers, writing elements, paper drives and power supplies. Different heads of water were applied to the transducers for calibration of transducers and recorder.

Brass casings were made to waterproof the transducers. Provision was made to release trapped air in the

casing through a screw control.

c) X-ray Apparatus -- The X-ray apparatus used in this research work is commercially called a Fedrex X-ray 140 kV, which was made in Copenhagen, Denmark. The apparatus consisted of two units, namely, the source unit containing the high tension filament transformer and X-ray tube, and the control unit containing controls, switches, and measuring devices. The apparatus was operated on 110 volts at 60 cycles with a power consumption of 1.5 kilovolt-amps. The voltage supplies to the tube were regulated steply from 30 kilovolts to 100 kilovolts and/or from 70 kv to 130 kv. The tube current was regulated from 0 to 4 milliamps. All the pictures taken in the tests were on tube voltage of 120 kv, tube current of 4 mA, and exposure time of 20 seconds.

The anode angle was approximately 20° and, by suing the principle of line focus, an effective focal spot of 1.5 mm. was obtained. (Fig. 7)

D) X-ray Film -- The film was Kodak Industrial X-ray, type KK35mm Roll film, and was cut into rectangular shapes of 1-1/4" x 7-1/2".

E) Film Holder -- The film holder was made of two pieces of cardboard (1-1/2" x 7-1/2") sandwiching a black paper envelope which kept the film dark. Two pieces of 0.005 inch thick lead screens, facing each other, were stuck on the inside of the paper envelope, so that

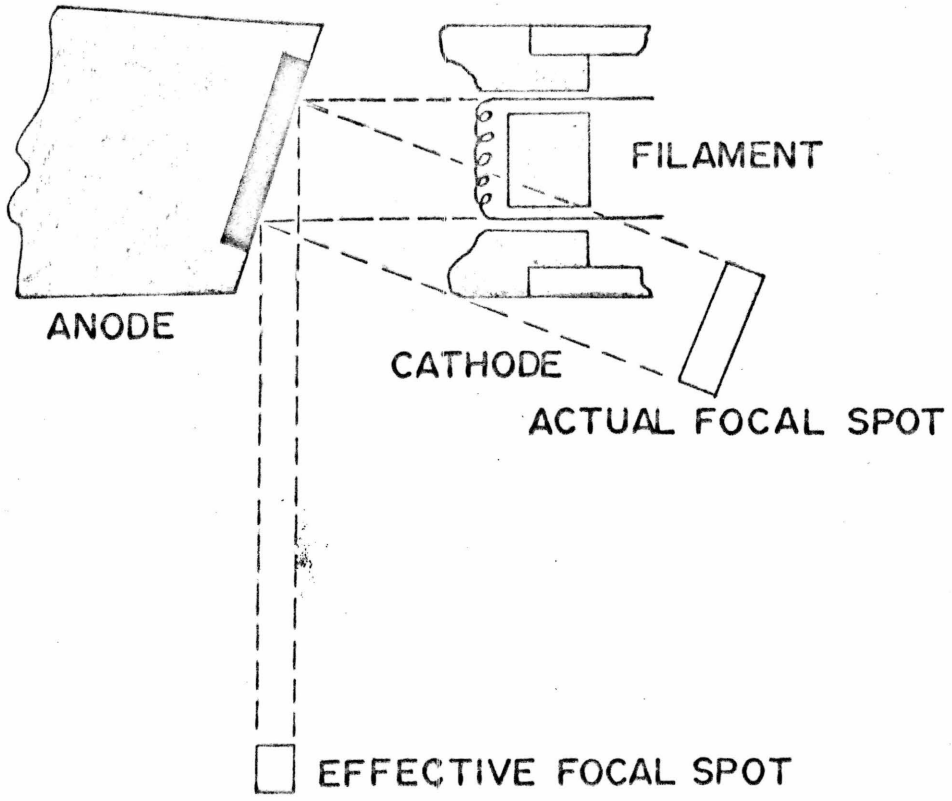

FIG. 7 DIAGRAM OF A LINE-FOCUS TUBE DEPICTING RELATION BETWEEN ACTUAL FOCAL SPOT AND EFFECTIVE FOCAL SPOT, AS PROJECTED FROM A 20° ANODE (AFTER KODAK, 1957)

when the paper envelope was closed the lead screens were in direct contact with the film. The lead screens absorbed the longer wavelength scattered radiation more than the primary radiation and intensified the latter more than the former. (Lo, 1964) the holder, after being loaded, was enveloped with a membrane and was secured with a rubber band. It was inserted into the water and was attached on the window of the cylinder where horizontal lead solders were set as reference lines.

F) Marker -- Four pieces of lead solder with 0.015" diameter were soldered together to form a cross; these crosses were used as markers and located horizontally along the center line of the sample, approximately half inch apart vertically.

Preparation of Sample

The soil sample used in this research work was amorphous-granular peat, which was obtained two feet below the surface of a lake near Parry Sound, Ontario. This material is dark grey in colour and is composed of fine organic fibers and mineral particles. The vegetal cover is classified as FI (Radforth, 1952). The water content of the sample before testing was in the region of 550 to 650% of the dry weight. Its specific gravity was within the range of 2.2 to 2.3. The liquid limit was 400%, and the plastic limit was 170%. The ignition loss was 25.5 of oven dried weight.

After being remoulded by mixing (in order to have a homogeneous sample), the peat was poured slowly into the consolidometer. It was sampled layer by layer. A lead marker was placed on top of each layer which was about half an inch in thickness.

Before the load increment was applied to the sample, it had been consolidated under certain pressure (such as the loading piston itself, or the piston plus another appropriate loading) for a certain time which was three days beyond the time required for the total dissipation of the pore water pressure of the sample. The purpose of this kind of sampling was to obtain a sample as homogeneous as possible.

Testing Procedure

The settlements of the top surface of the sample were measured by a dial gauge; these were taken as references to determine the time interval for taking X-ray pictures that showed the settlements of the layers. The X-ray pictures after being developed were read by a porta trace which could read the displacements of the markers to the nearest 1/64 of an inch. For every load increment, the X-ray pictures were taken until the pore water pressures were dissipated out. The tests were terminated when the trends of the variation of total pressure and the rate of secondary consolidation could be determined.

The data of pore water pressures and of total pressures recorded by Beckman recorder were obtained with calibrating factors.

CHAPTER 5

DATA ANALYSIS

Pore water pressure measurements of transducers #1, #2, #3 and #4, and total pressure measurements at the bottom of the sample, P_B, were obtained during the consolidation process. These measurements are shown in Fig. 8 and Table I, Appendix A, which also shows the settlements at the top of the sample. Positions of the four markers, A, B, C and D during consolidation were obtained from X-ray radiographs. The results are shown in Table II after the correction of X-ray parallax was made. (Fig. 9)

By extrapolating the data obtained in transducers #1, #2, #3 and #4, pore pressure isochrones were constructed, which are shown in Fig. 10. The pore pressure isochrones are the pore pressure profiles for various times. The hydraulic gradient (i) for any position at any time may be calculated for the pore pressure isochrones. The hydraulic gradients at the positions of the markers at any time are shown in Table II.

At the end of the consolidation test, the water-contents of the sample at upper, middle, and lower portions were found to be 197.78%, 193.59%, and 193.59% respectively.

FIG. 8

PRESSURE MEASUREMENTS

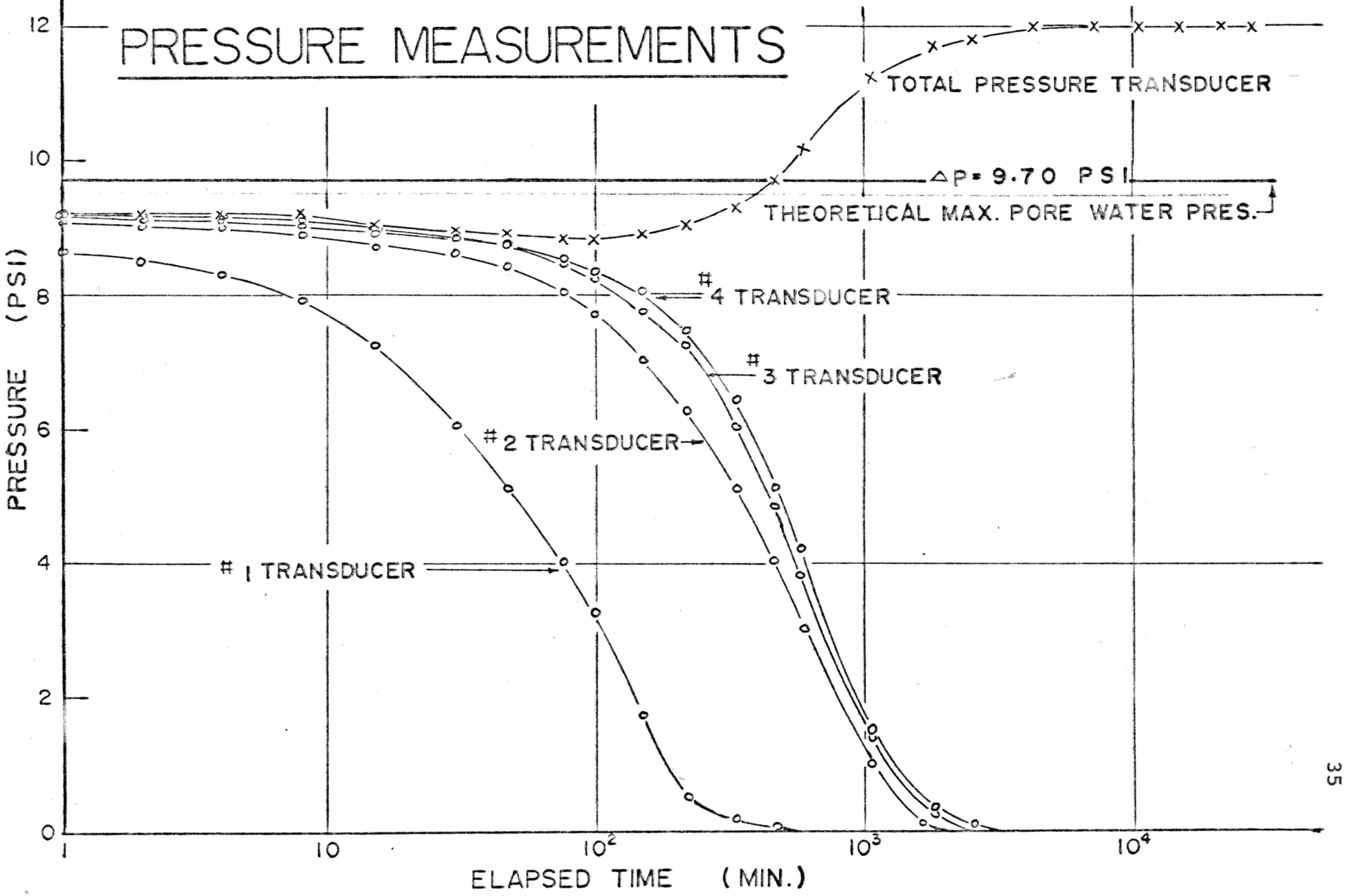

FIG. 9
SETTLEMENT CURVES

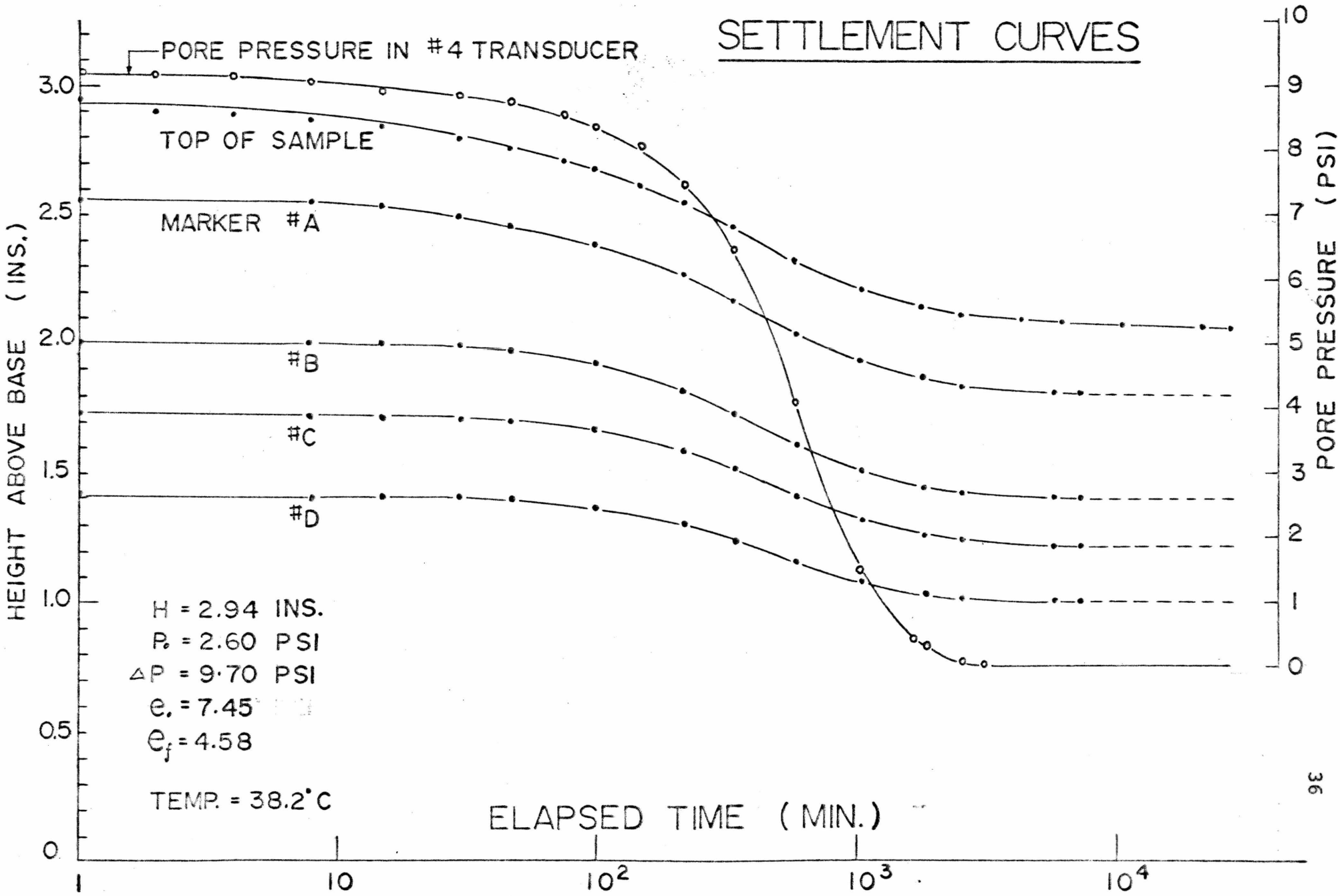

The average value of water content was 195.08%. Multiplying the average water content of peat by its specific gravity (2.30) the average void ratio of the peat sample at the end of the test was 4.487. The soil sample was assumed homogeneous before the load increment was applied. The thickness of the solid particles, z_o, of the sample was calculated as 0.375" from the final sample height of 2.056" and the final void ratio of 4.487.

The soil layer between marker A and marker B was named Zone AB, similarly, Zone BC and Zone CD. The thickness of the solid particles of Zone AB (Z_{AB}) compared with the total thickness of the solid particles of the whole sample (z_o), has the same ratio as the thickness of Zone AB at time t=o $\left[L_{AB} (z,o) \right]$, compared with the original thickness of the sample $\left[L(z_o,o) \text{ or } H \right]$. The thickness of the solid particles in Zone AB, Zone BC, and Zone CD were calculated as 0.0676", 0.0377", and 0.0392" respectively. Knowing the thickness of the solid particles and knowing the changes in thickness of layers for various time intervals, the changes in void ratio (Δe) for these time intervals of each layer were calculated and are shown in Table III.

The permeability of Zone AB over the time interval from t_1 to t_2 ($\Delta t = t_2 - t_1$) was calculated according to the formula

$$K = \frac{\Delta L'}{\Delta t \ \Delta i} \ ,$$

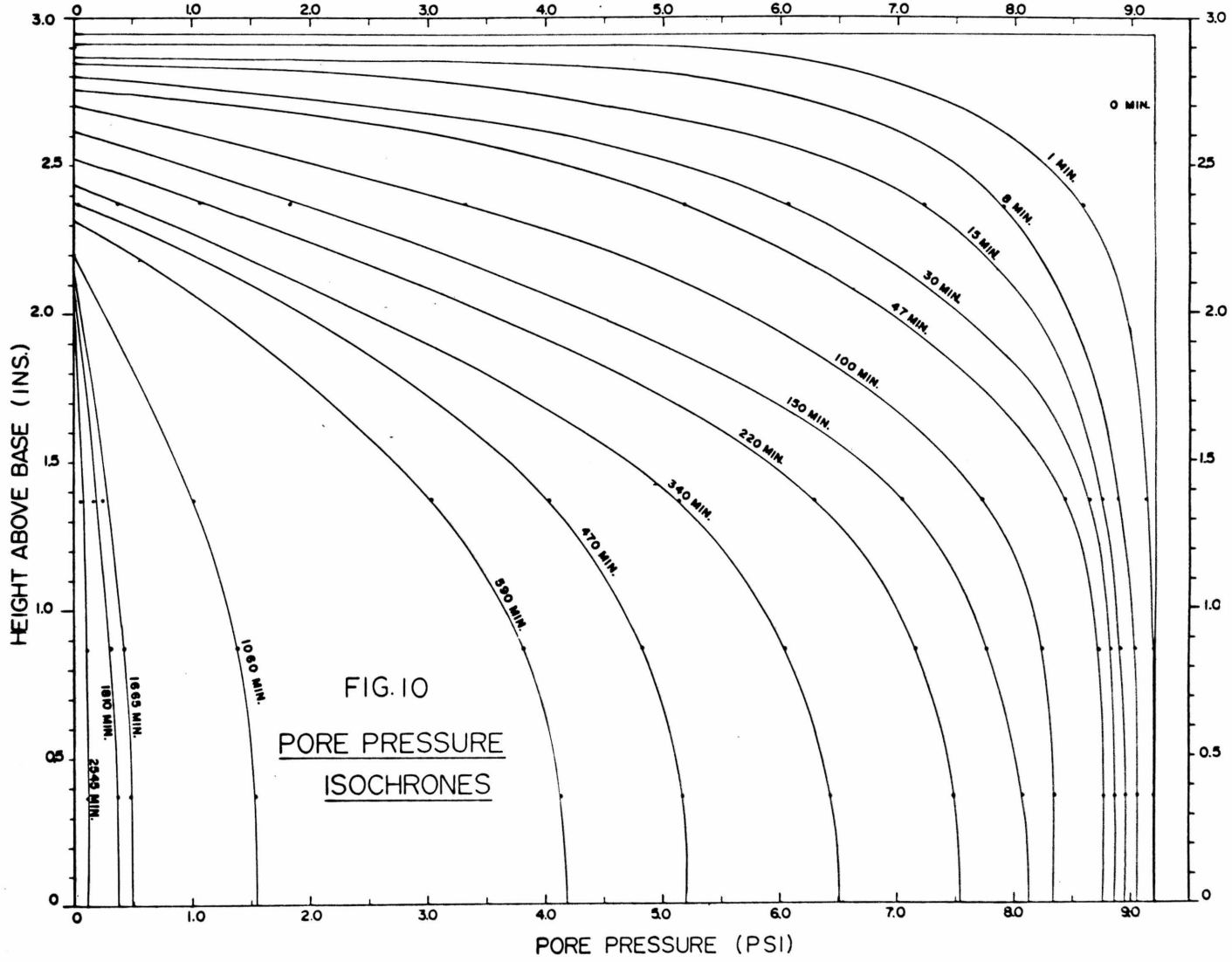

FIG. 10

PORE PRESSURE ISOCHRONES

where $\Delta L'$ is the change in depth of Zone AB over the time interval Δt. Δi is the average difference between the hydraulic gradients, which equals

$$\frac{\left[i_A - i_B\right]_{t_1} + \left[i_A - i_B\right]_{t_2}}{2} .$$

$\left[i_A - i_B\right]_{t_1}$ was the difference between the hydraulic gradients at the positions of markers A and B at time t_1.

Total pressure measurements were obtained during the test. P_T, the total pressure at the top of the sample applied by the piston equaled 9.70 psi. P_B, the total pressure at the bottom of the sample, varied with time. (Fig. 8) As the change in total pressure through the thickness and across the area was unknown, an assumption was made that the total pressure varied linearly through the thickness of the sample and was uniform over the area, (a discussion of this is presented in Chapter 6). Determining the total pressures at the positions of markers for various times by assuming the linear distribution from the obtained data (P_T and P_B), and determining the pore-water pressures at these positions, obtained from the pore pressure isochrones, average effective pressures for each zone over the time interval were obtained.

Table III and Table IV show the data of void ratio (e), permeability (k) and effective pressure(P'). This data were plotted in Fig. 11 and Fig. 12.

FIG. 11 e – LOG P' CURVES

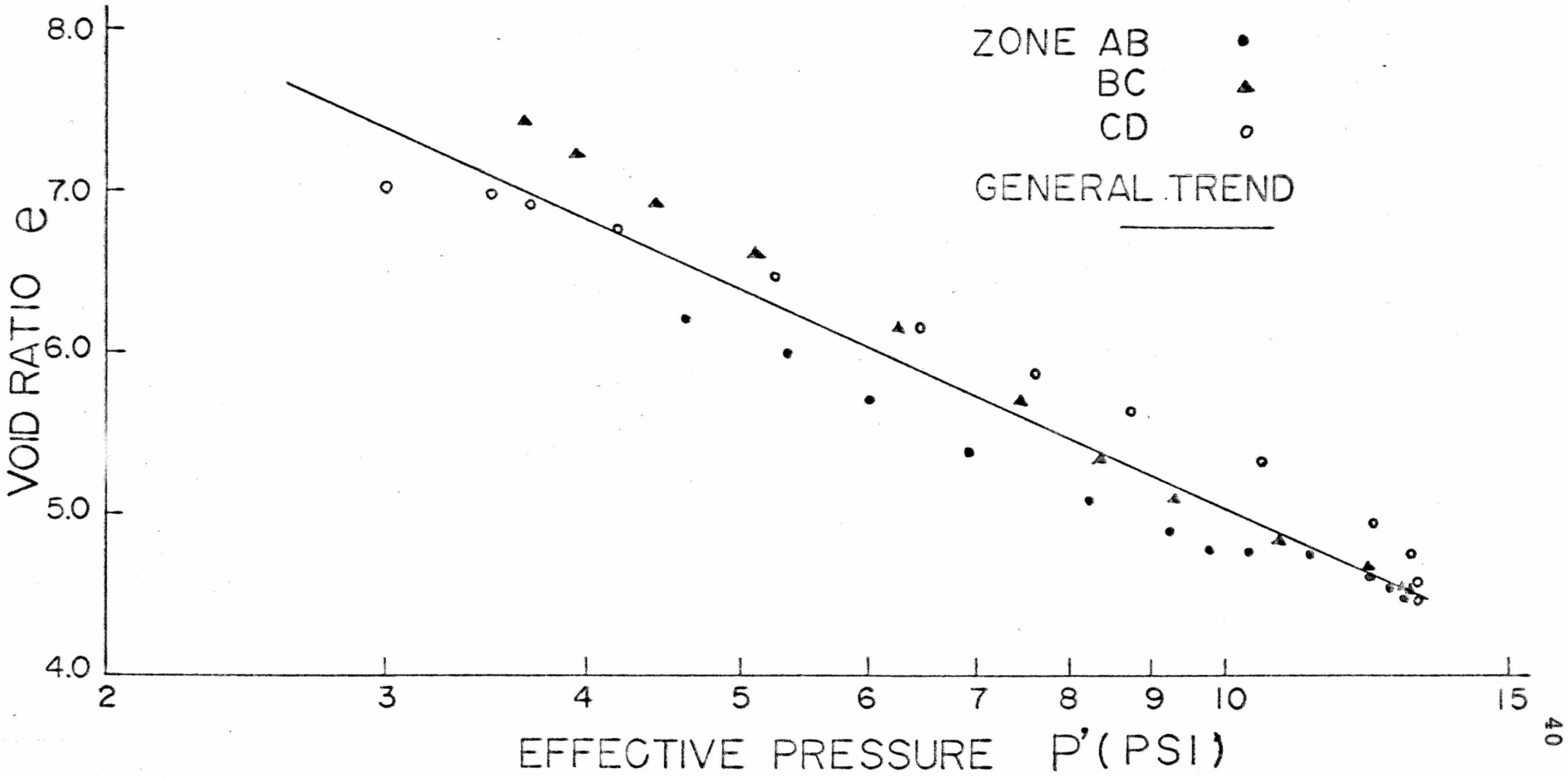

FIG.12 e-LOG K CURVE

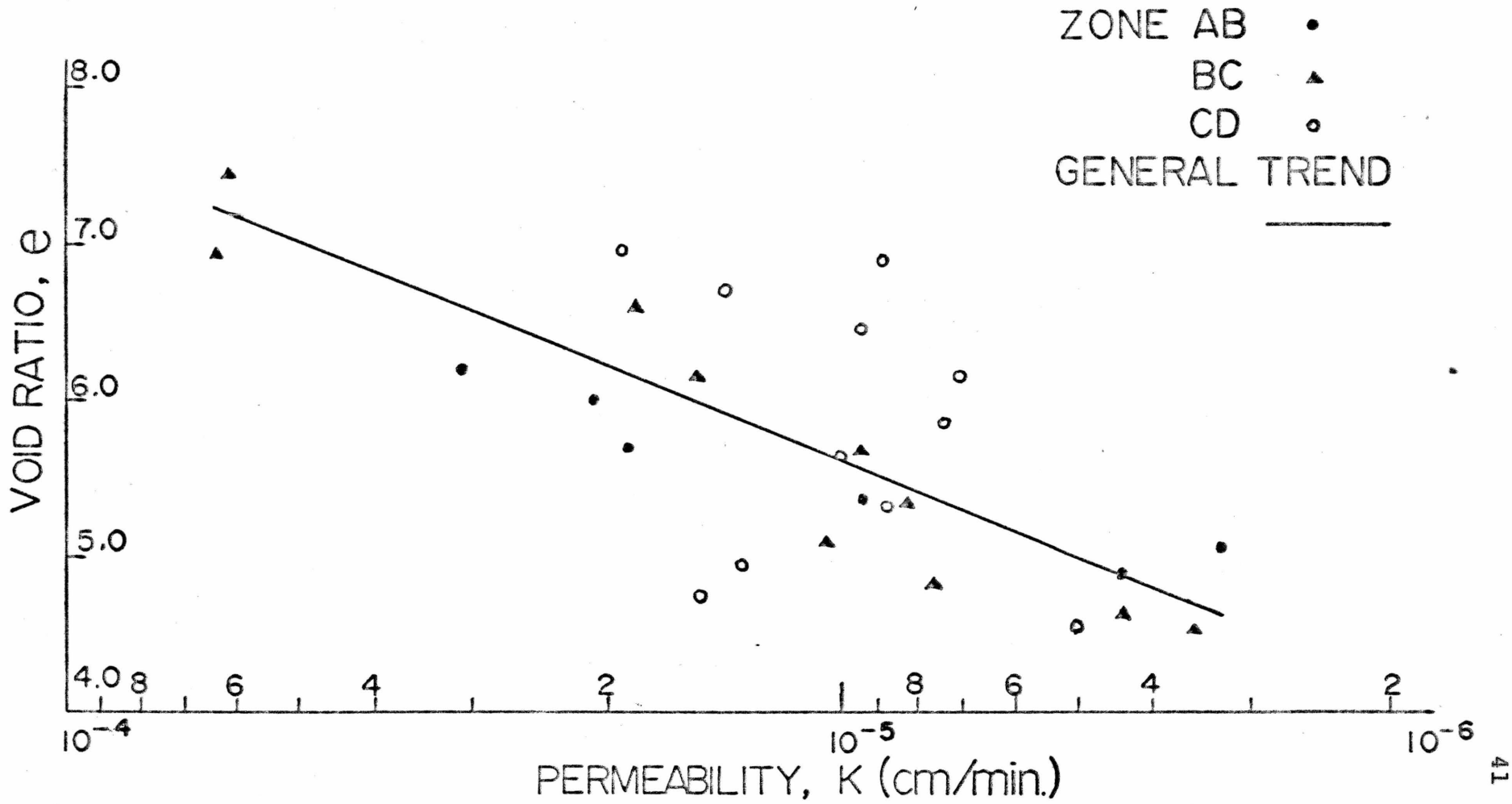

In order to find the Flow-Loading Parameter (θ) of peat, a relationship between Log $\left(\frac{k}{1+e} \Big/ \frac{k_1}{1+e_1} \right)$ and Log $\left(\frac{P'}{P'_1} \right)$ was required. k_1, e_1 and P'_1 are the permeability, void ratio and effective pressure at the starting time of measurement. Plotting the values of the general relationships of e-log P' and e-log k, a general trend of Log $\left(\frac{k}{1+e} \Big/ \frac{k_1}{1+e_1} \right)$ versus Log $\left(\frac{P'}{P'_o} \right)$ was obtained; the data were shown in Table V and plotted graphically in Fig. 13. θ was found to be 61^o.

The general relationships between P', e, k and $\frac{k}{1+e}$ are shown in Table VI.

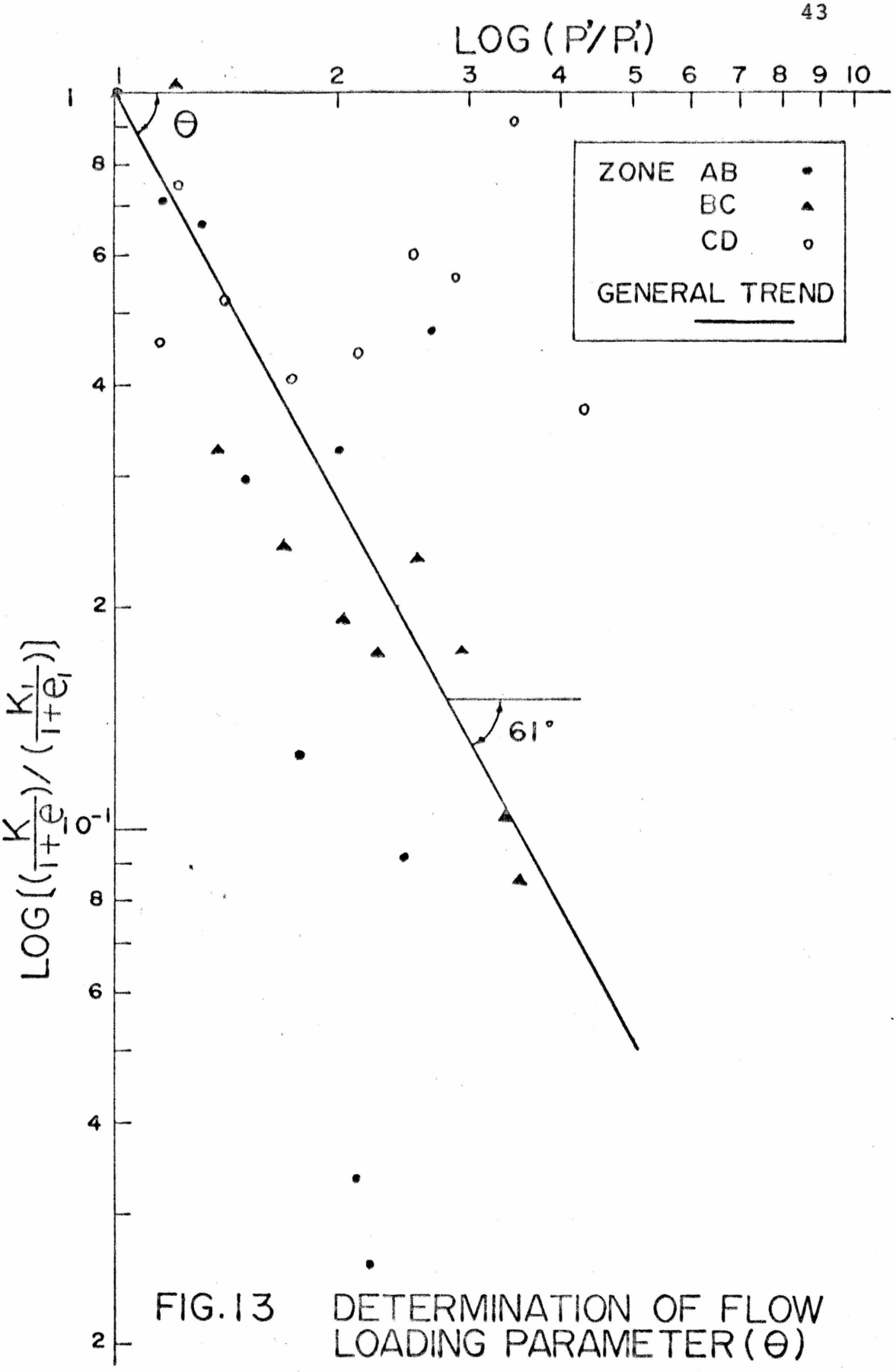

FIG. 13 DETERMINATION OF FLOW LOADING PARAMETER (θ)

CHAPTER 6

DISCUSSIONS ON THE EXTENDED THEORY

This research was conducted to investigate some fundamental properties of peat, from which an extended theory governing the one-dimensional consolidation of soil could be derived. In order to demonstrate the validity of the theory, the basic assumptions necessary for the derivation were investigated:

1) The assumption of a linear relationship between the void ratio (e) and the logarithm of effective pressure (log P') is justified by Fig. 11. The scattering of different zones on the e-log P' curve can be attributed to:

a) The variation of the property of peat itself; (Hanrahan, 1954)

b) The viscous or plastic deformation of the soil during the consolidation process, which could not be considered in the primary consolidation theory; this theory treats the soil skeleton as an elastic body;

c) The non-planar strain which could be caused by non-uniformly distributed effective pressures over the area of the sample; the boundary of the consolidometer and

the unknown distribution of frictional force along the cylinder wall could cause a deviation from the plane strain condition.

As far as the whole soil sample is concerend, a straight line relationship between e and log P' is shown to be valid in Fig. 11.

2) A linear relationship between the void ratio (e) and the logarithm of permeability (log k) is shown in Fig. 12.

3) The relationship between the effective pressure and its corresponding void ratio and permeability are assumed to be

$$\frac{k_1}{1+e_1}(P_1')^{\tan\theta} = \frac{k_2}{1+e_2}(P_2')^{\tan\theta}$$

or

$$\log\left(\frac{k_1}{1+e_1} \Big/ \frac{k_2}{1+e_2}\right) = -\tan\theta \log\left(\frac{P_1'}{P_2'}\right)$$

where k_1 and e_1 are the permeability and void ratio corresponding to the effective pressure P_1'. θ is the Flow-Loading Parameter representing the behaviour of the soil during consolidation. Fig. 13 shows this relationship. The scattering between the zones may be inherited from Fig. 11 and Fig. 12. Combining the data for the general relationships of e-log P' (Fig. 11) and e-log k (Fig. 12),

a straight line relationship was obtained on the $\log \left(\frac{k}{1+e} / \frac{k_1}{1+e_1} \right)$ - $\log\left(\frac{P'}{P'_1}\right)$ graph (Fig. 13); the Flow-Loading Parameter (θ) was found to be 61°. For different soils, the parameter θ may be different. Therefore, in dealing with consolidation, this parameter may be one of the major factors. The value of $\frac{k}{1+e}$ in theequation of continuity Eq.(1) was taken as a constant during the consolidation process by Terzaghi. However, Fig. 13 shows:

a) For small load increments,that is, P/P_1 is nearly 1, the change in $\frac{k}{1+e}$ is small no matter what θ is. Therefore, the simplification of Terzaghi by taking $\frac{k}{1+e}$ as a constant during the consolidation process is acceptable for small load increment ratios.

b) For large load increment ratio, the change in $\frac{k}{1+e}$ becomes significant for large values of θ. However, for small values of θ, this change becomes insignificant.

c) The change in $\frac{k}{1+e}$ increases as load increment ratio or/and the Flow-Loading Parameter (θ) increases.

4) A general theory was derived basically depending on the soil properties discussed previously. Curves were plotted relating both the Degree of Consolidation (S) and the Dissipation of Maximum Pore-water Pressure (U) to the classical Time Factor (T). (Fig. 14 and Fig. 15) The effects of the load increment ratio (Δ) and the Flow-Loading Parameter (θ) can be seen on these graphs. The influence of these parameters can be compared to the

FIG. 14 THEORETICAL CURVES OF DEGREE OF CONSOLIDATION FOR VARIES VALUES OF THE FLOW-LOADING PARAMETER(Θ) AND LOAD INCREMENT RATIO(Δ)

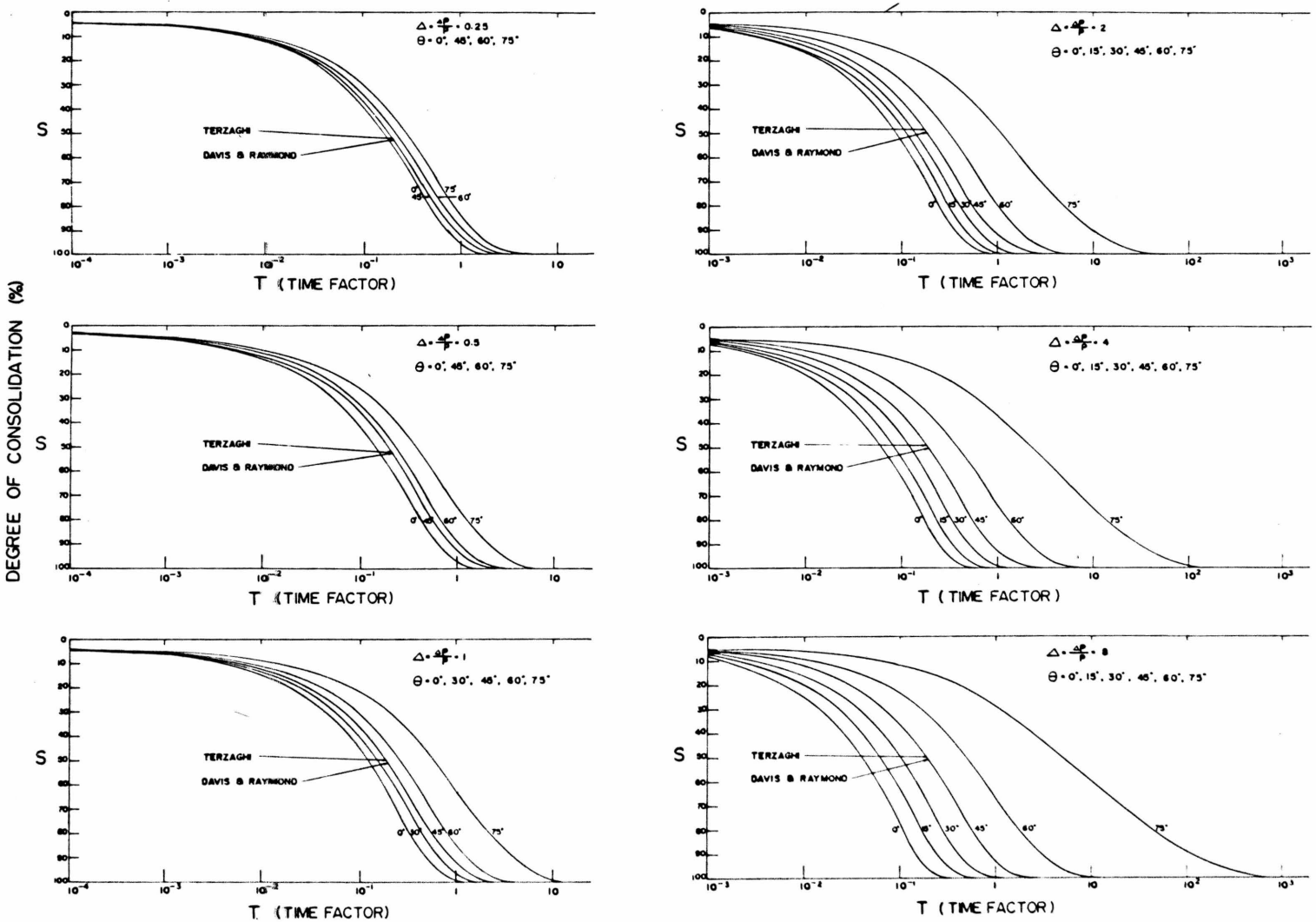

FIG. 15 THEORETICAL CURVES OF PORE PRESSURE DISSIPATION AT THE SAMPLE BOTTOM(X=1) FOR VARIES VALUES OF THE FLOW-LOADING PARAMETER(θ) AND LOAD INCREMENT RATIO(△)

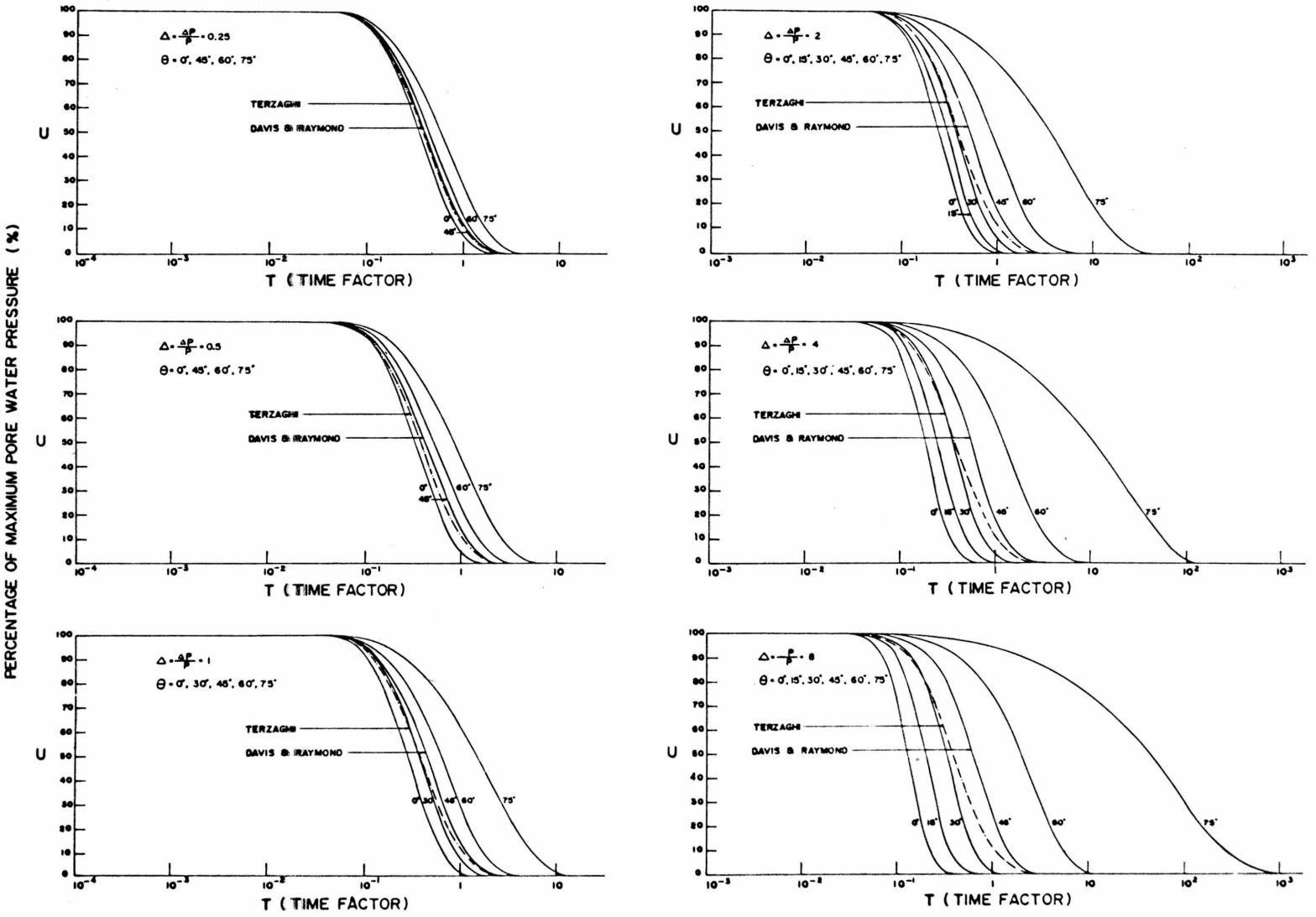

Terzaghi Theory (dotted line) which was assumed to be independent of these parameters, and the theory by Davis and Raymond (1965) which happens to coincide with the special case of $\theta=45^{\circ}$. Various values of the load increment ratio (Δ) were chosen as 0.25, 0.5, 1, 2, 4, 8. The chosen values of the Flow-Loading Parameter (θ) are 0°, 15°, 30°, 45°, 60°, 75°.

The influences of the load increment ratio (Δ) and the Flow-Loading Parameter (θ) on the degree of consolidation and on the dissipation of pore water pressure at the bottom of the sample are shown in Fig. 16 and Fig. 17. For small load increment ratios, that is, an increase in effective pressure which is small relative to the initial effective pressure, the influence of the Flow-Loading Parameter (θ) on the degree of consolidation and on the dissipation of pore-water pressure is small for values of θ from 0° to 75°. (Fig. 16) This indicates that, for a small load increment ratio, the consideration of the ratio $\frac{k}{1+e}$ as a certain constant value during the consolidation process is acceptable. This consideration was made by Terzaghi when he derived his classical consolidation theory. However, as the load increment ratio increases, the influence of θ becomes greater. This indicates that when the increase in effective pressure is large relative to the initial effective pressure in the consolidation

FIG. 16 INFLUENCE OF LOAD INCREMENT RATIO (Δ)

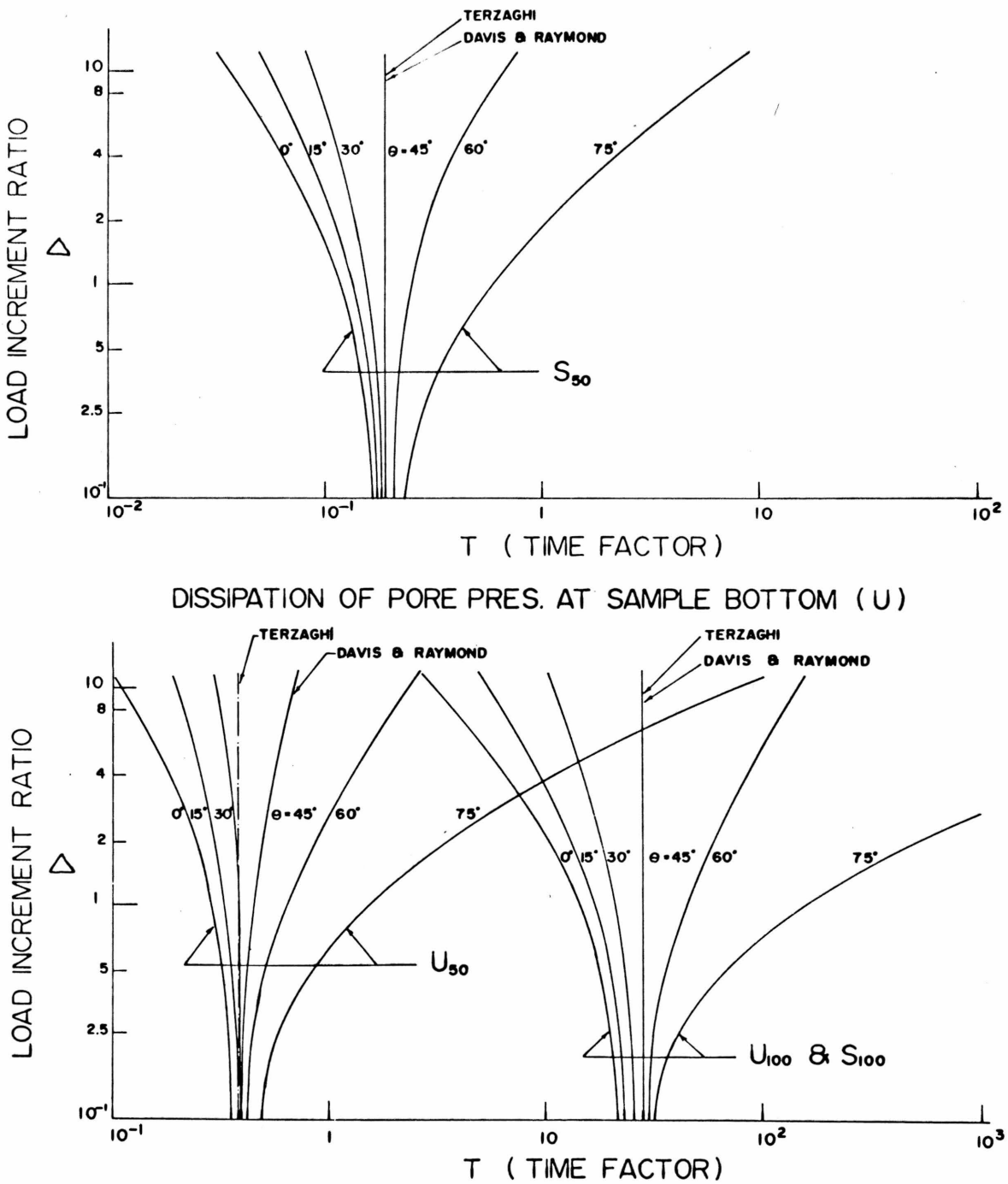

FIG. 17 INFLUENCE OF FLOW-LOADING PARAMETER (Θ)

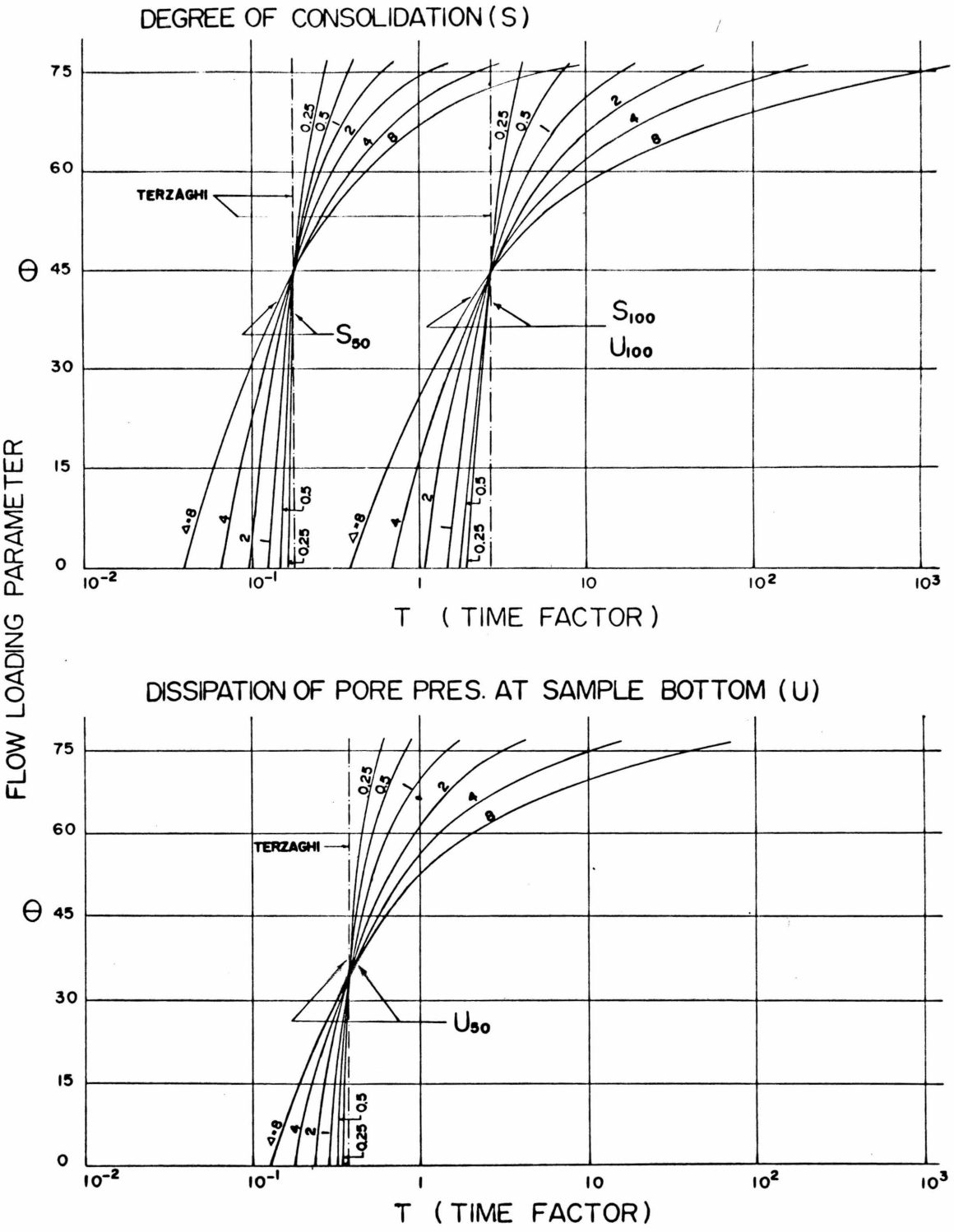

process, the interaction between the permeability (k), void ratio (e) and effective pressure(P') becomes significant. Therefore, for larger load increment ratios, the degree of consolidation and the dissipation of pore-water pressure are affected not only by the load increment ratios but also by the Flow-Loading Parameters which relate the void ratio (e), permeability (k) and effective pressure (P'). (Fig. 16)

Fig. 17 shows that the time for degrees of consolidation of 50% and 100% is independent of load increment ratio when θ equals 45°. When θ is greater than 45°, the time increases as the load increment ratio increases; when θ is smaller than 45°, the time decreases as the load increment ratio increases. The dissipation of pore water pressure has a similar trend. (Fig. 17)

5) In order to make a comparison between this extended theory, the David and Raymond theory, and the Terzaghi theory, the experimental data were plotted into S-log T, and U-log T curves, according to each of the theories. The dimensionless parameters are Degree of Consolidation (S), Dissipation of Maximum Pore-water Pressure (U) and Time Factor (T); these are plotted in Fig. 18 and Fig. 19.

The experimental data were fitted at S=50%, and U=50%. It is noted that according to the definition of a

FIG. 18 COMPARISONS OF EXPERIMENTAL DATA TO PREVIOUS THEORIES

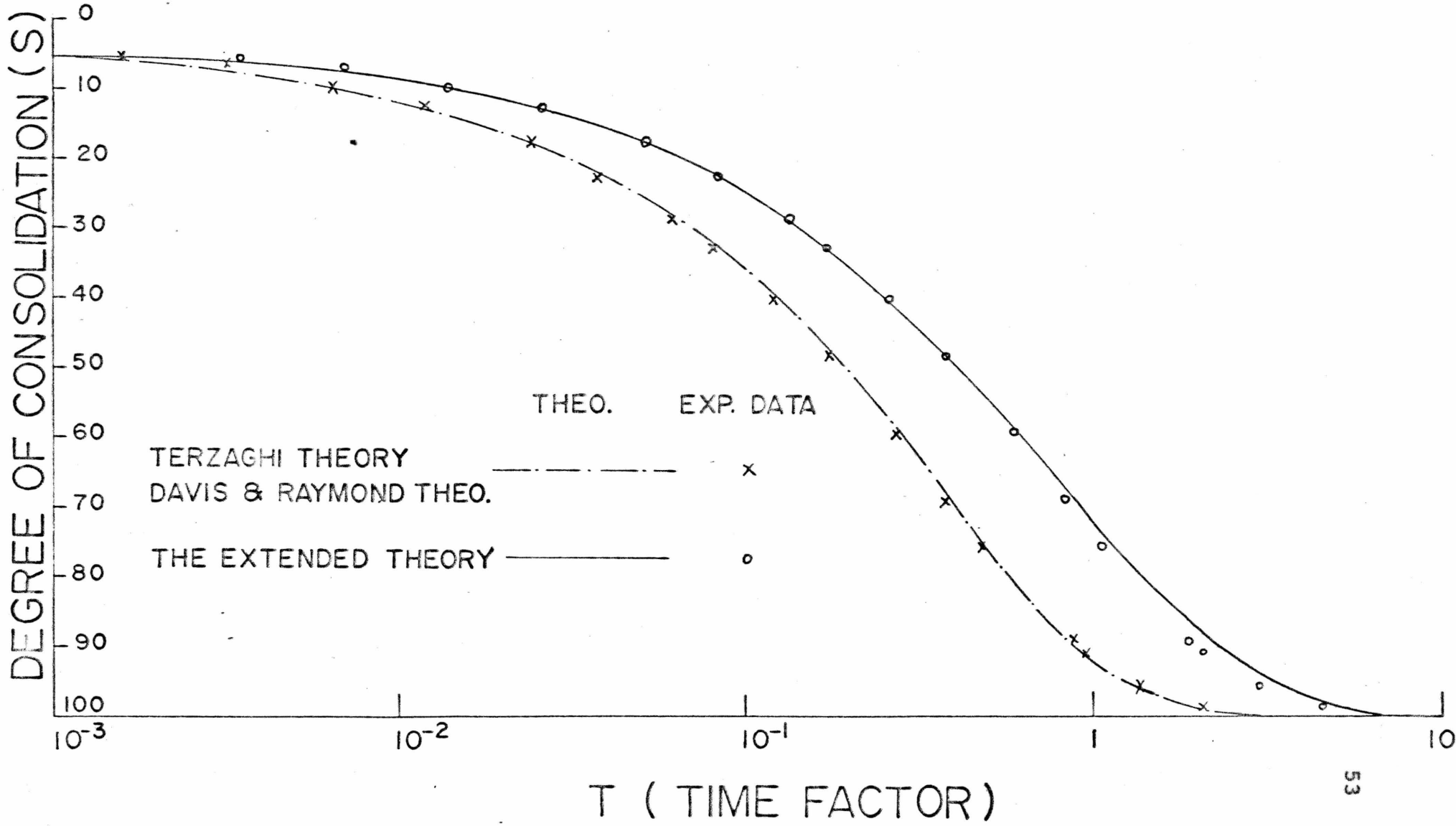

FIG.19 COMPARISONS OF EXPERIMENTAL DATA TO PREVIOUS THEORIES

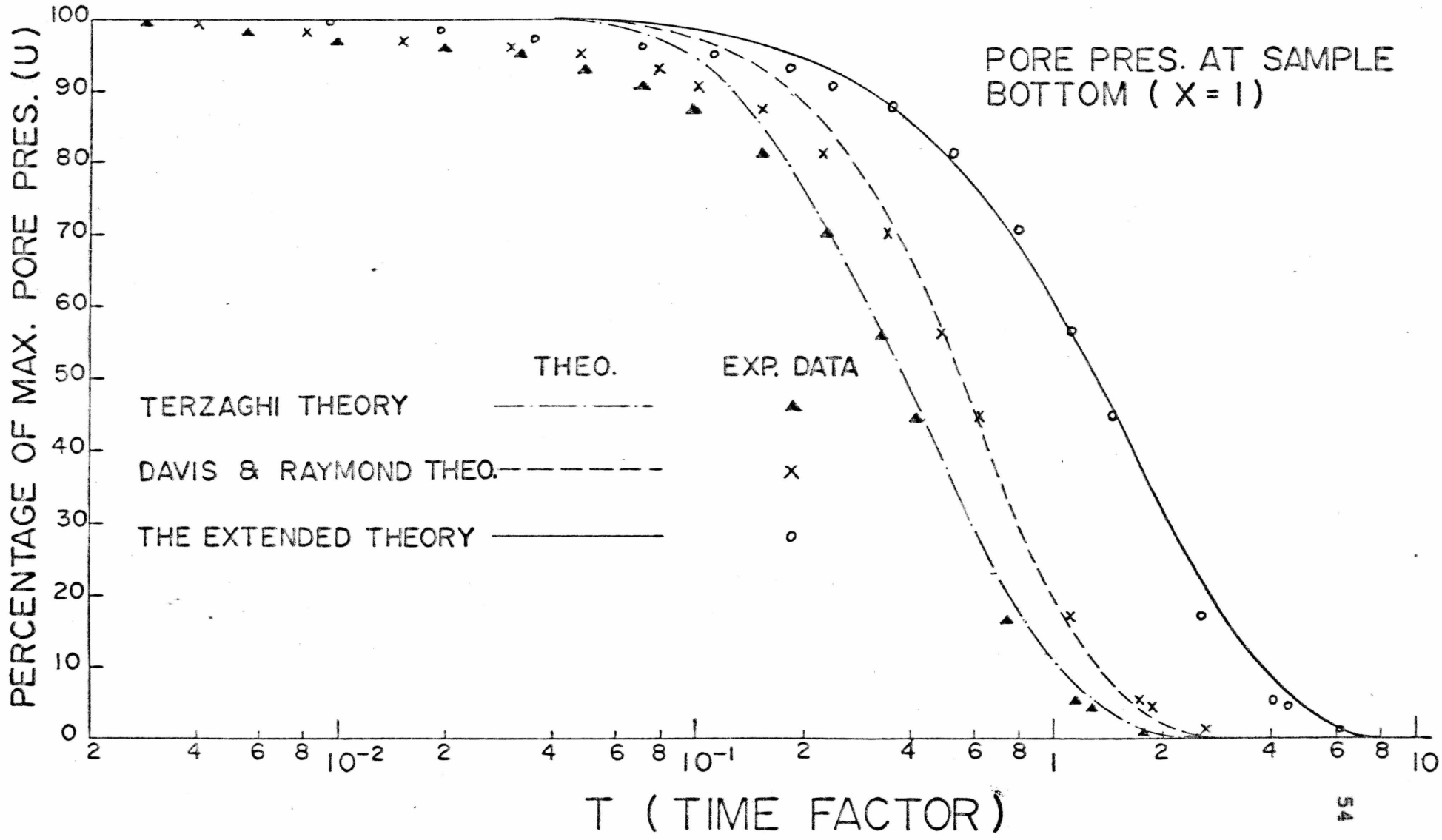

best fitting curve, the general theory fits the experimental data.

6) The total pressure at the center of the bottom of the soil sample was measured. Fig. 8 shows the variation of total pressure during the consolidation process. The total pressure was measured as 9.20 psi at the instant of the load increment application which produced a piston loading of 9.70 psi over the top of the sample. The frictional resistance between the cylinder wall and the soil may be one of the reasons causing the difference between the measured (9.20 psi) and the anticipated (9.70 psi) values. The total pressure decreased to a value of 8.82 psi (about 96% of the initial value) when the pore water pressure at #4 transducer reduced to 93% of its initial (maximum) value. Following that, the total pressure increased until the end of the primary consolidation, reaching the maximum value of 12.00 psi. After the pore water pressure dissipated, the total pressure remained at the constant value of 12.00 psi. The total pressures over the bottom of the sample are generally uniform during the early stages of consolidation. As the pore water pressure dissipates, the distribution becomes more non-uniform. Fig. 20 describes the possible pressure distribution over the bottom area of the sample. The total forces on the sample bottom are represented by A_f and B_f in Fig. 20. The force represented by A_f is equal to the force

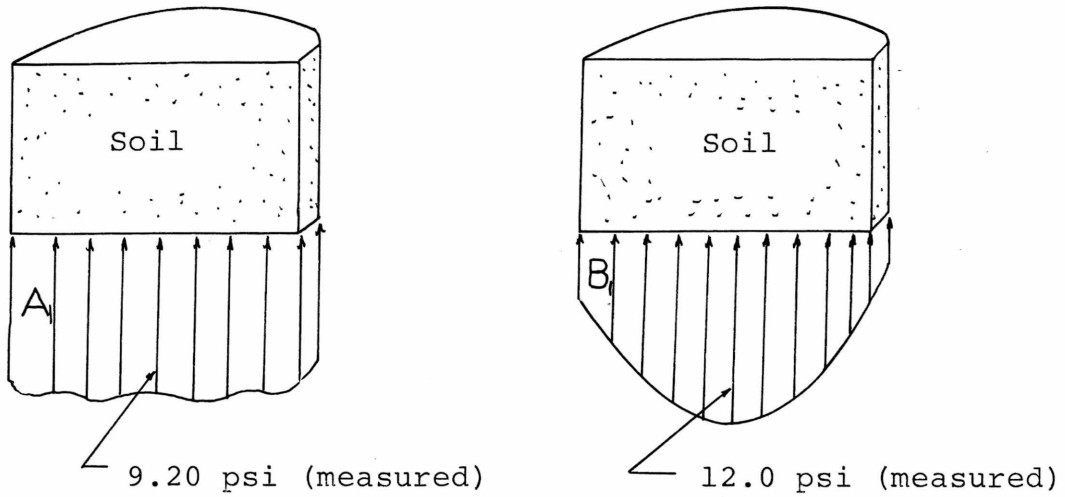

Fig. 20 Pressure Distribution on the Sample Bottom

represented by B_1, plus the force absorbed by the frictional resistance between the soil and the consolidometer.

The non-uniformly distributed total pressure during the later stages of the consolidation process, which is not compatible with the assumption of a uniformly distributed total pressure over any horizontal area within the soil sample, may be one of the reasons causing the scattering between the experimental data and the theoretical curves of degree of consolidation and dissipation of pore-water pressure. (Fig. 18 and Fig. 19)

7) Because of the geometrical confinement of the consolidometer on the soil sample, the validity of the

assumption of uniformly planar total pressure, which was made during the derivation of the consolidation theory, may be affected. Thus, an elementary study on the boundary conditions of the soil sample under consolidation is necessary.

When the primary consolidation is terminating, that is, when the pore water pressure has dissipated to almost zero, the properties of the soil are assumed to be elastic, homogeneous, and isotropic. The properties are Modulus of Elasticity (E), Modulus of Rigidity (G), and Poisson's ratio (v). If the theory of elasticity is applicable, the physical properties and the boundary conditions are:

Navier's Equation:-

$$E \frac{\partial^2 U_\gamma}{\partial \gamma^2} + G \left(\frac{\partial^2 U_z}{\partial \gamma \partial z} + \frac{\partial^2 U_\gamma}{\partial z^2} \right) - \frac{E}{\gamma} \left(\frac{\partial U_\gamma}{\partial \gamma} + \frac{U_\gamma}{\gamma} \right) = o$$

$$E \frac{\partial^2 U_z}{\partial z^2} + G \left(\frac{\partial^2 U_z}{\partial \gamma^2} + \frac{\partial^2 U_\gamma}{\partial z \partial \gamma} \right) + \frac{G}{v_\gamma} \left(\frac{\partial U_z}{\partial \gamma} + \frac{\partial U_\gamma}{\partial z} \right) = o$$

Boundary conditions:

(a) $U_z(\gamma, o) = o,$

(b) $\int_o^a E \frac{\partial U_z}{\partial z} (\gamma, L)\ 2\lambda\gamma d\gamma = -P,$

(c) $\int_o^a E \frac{\partial U_z(\gamma, o)}{\partial z} (\gamma, o)\ 2\lambda\gamma d\gamma$

$$= -P + \int_o^L \left(-f \frac{\partial U_\gamma(a, z)}{\partial \gamma} E\ 2\lambda a \right) dz,$$

$$(d)\quad U_\gamma(a,z) = o,$$

$$(e)\quad U_\gamma(o,z) = o,$$

$$(f)\quad T_{z\gamma}(a,z) = G\left(\frac{\partial U_\gamma(a,z)}{\partial z} + \frac{\partial U_z(a,z)}{\partial \gamma}\right)$$

$$= -f \cdot \frac{\partial U_\gamma(a,z)}{\partial \gamma} E,$$

$$(g)\quad T_{\gamma z}(\gamma,o) = G\left(\frac{\partial U_\gamma(\gamma,o)}{\partial z} + \frac{\partial U_z(\gamma,o)}{\partial \gamma}\right)$$

$$= -f_1 \frac{\partial U_z}{\partial z}(\gamma,o)\ E$$

$$(h)\quad T_{\gamma z}(\gamma,L) = G\left(\frac{\partial U_\gamma(\gamma,L)}{\partial z} + \frac{\partial U_z(\gamma,L)}{\partial \gamma}\right)$$

$$= -f_2 \frac{\partial U_z}{\partial z}(\gamma,L)\ E$$

where

U_z is the displacement of the soil particles in z (vertical) direction;

U_γ is the displacement in γ (radial) direction;

f, f_1, f_2 are the coefficients of friction between the soil sample and the wall, base, and the piston respectively.

P is the total force acting on the loading piston which imposes a uniformly distributed pressure ($p=\frac{P}{A}$) on the top of the sample; where A is the area of the piston. Fig. 21 is a diagramatic sketch of the stress conditions.

Because of complicated boundary conditions, the displacement functions, from which the stress conditions can be obtained, were unable to be solved analytically. However, the stress is not a uniformly planar stress $\frac{\partial}{\partial \gamma}\frac{\partial U_z(\gamma,z)}{\partial z} = o$ because of the shearing stresses ($T_{\gamma z}(a,z)$) acting along the

walls. Because of the viscous property of the soil skeleton, the stress distribution within the soil during consolidation is unknown. The non-uniform distribution of total pressures over the bottom area obtained from the experimental data, shows that the assumption of planar stress and strain is not vindicated.

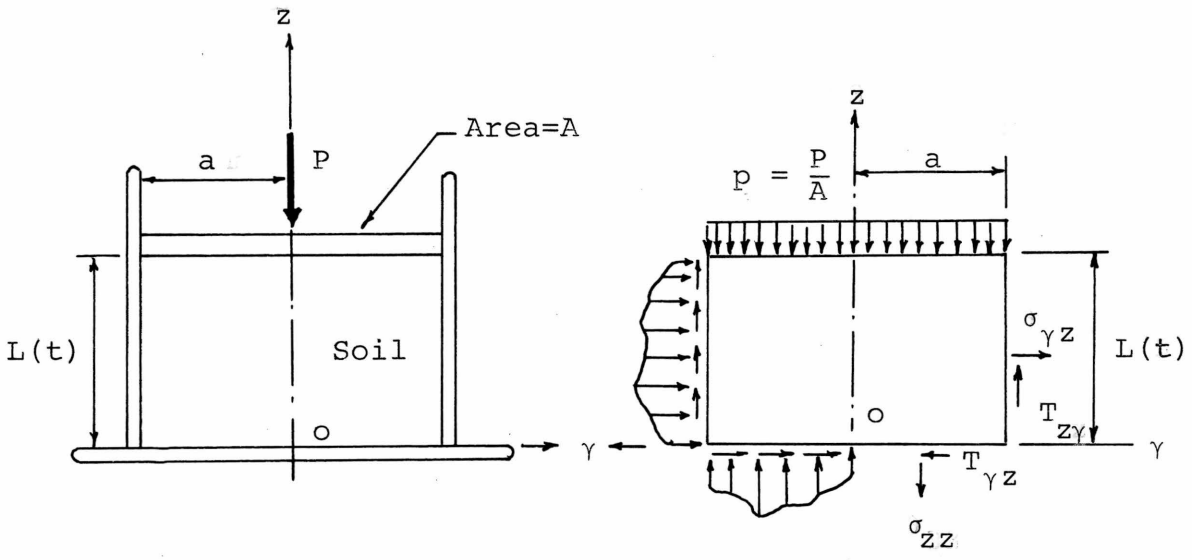

Fig. 21 A Diagramic Sketch of Stress Conditions

CHAPTER 7

CONCLUSIONS AND RECOMMENDATIONS

Conclusions

1) An extended theory was derived for one-dimensional consolidation with the assumption of planar stress and strain. In the theory, the change in the permeability and the change in the void ratio were taken into account.

2) For remoulded samples which are prepared in a consolidometer, the non-uniform distribution of the preconsolidated pressure inherently affects the soil properties of subsequent consolidation and shearing strength tests.

3) The boundary conditions of the consolidometer are not compatible with the field conditions. Besides the drainage condition, the increase of total pressure at the bottom center of the soil sample is contrary to the field conditions where the pressure distribution under a load increment decreases with depth.

4) Therefore, predictions from the consolidometer test to the field consolidation conditions are doubtful.

5) The significance of frictional resistance along the consolidometer walls has been investigated by

others (Leonards and Girault, 1961); this resistance can be minimized by increasing the ratio of sample diameter to depth. Therefore, it would be unsuitable to have a thick soil sample for the consolidometer test, because of the introduction of frictional force along the wall.

Recommendations

1) It is recommended that further investigations on the boundary pressure distribution of the soil sample within the consolidometer are needed. The assumption of planar stress and planar strain in the theories of consolidation needs further justification.

2) A study on field drainage conditions may evaluate the merits of the application of the consolidometer.

3) Investigations on the Flow-Loading Parameters for various kinds of soil are needed.

4) Further study, combining the primary and secondary consolidation effects should lead to the understanding of the consolidation process.

REFERENCES

Abbott, M. B. (1960). "One dimensional consolidation of multilayered soils"; Geotechnique, Vol. X, p.151.

Barden, L. (1965). "Consolidation of clay with non-linear viscosity"; Geotechnique, Vol. XV, No. 4, December 1965, p.345.

Biot, M. A. (1941). "A general theory of one dimensional consolidation of soils"; Journal of Appl. Phys., Vol. 12.

----------. (1956). "Theory of deformation of a porous viscoelastic anisotropic solid"; Journal of Appl. Phys., Vol. 17.

Brawner, C. O. (1961). "The compressibility of peat with reference to the construction of a major highway in B.C."; Proc. 7th Muskeg Research Conf., N.R.C, T.M. No. 71, p.204.

Buisman, A. S. K. (1936). "Results of long duration settlement test"; Proc. ICOSMFE I, Vol. I, p.103.

Casagrande, A. (1936). "The determination of the pre-consolidation load and its practical significance"; Proc. ICOSMFE I, Vol. III, p.66.

Davis, E. H. and Raymond, G. P. (1965). "A non-linear theory of consolidation"; Geotechnique, Vol. XV, No. 2, June 1965, p.161.

Enright, C. T. and Adams, J. I. (1963). "A comparison of field and laboratory consolidation measurements in peat"; Proc. 9th Muskeg Research Conf.

Gibson, R. E. and Lo, K. Y. (1961). "A Theory of Consolidation of Soils Exhibiting Secondary Compression," Publication No. 41, Norwegian Geotechnical Inst., Oslo.

Hanrahan, E. T. (1954). "An investigation of some physical properties of peat"; Geotechnique, Vol. IV, p.108.

Hansen, J. B. (1961). "A model law for simultaneous primary and secondary consolidation"; ICOSMFE V, Vol. I, p.133.

Kapp, M. S., discussion of "Report of Consolidation Tests with Peat," by J. B. Thompson and L. A. Palmer, Special Technical Publication No. 126, Symposium on Consolidation Testing of Soils, ASTM, June 1951, p.8.

Koppejan, A. W. (1948). "A formula combining the Terzaghi load compression relationship and the Buisman time effect"; Proc. ICOSMFE II, Vol. II, p.32.

Lake, J. R. (1961). "Investigations of the problem of constructing roads on peat in Scotland"; Proc. 7th Muskeg Research Conf., N.R.C., T.M. No. 71, p.133.

Lea, N. D. and Brawner, C. O. (1959). "Foundation and Pavement Design for Highways on Peat," Presented at 40th Convention of the Canadian Good Roads Assn., Vancouver, B.C., September 1959.

Leonards, G. A. and Girault, P. (1961). "A study of the one-dimensional consolidation test"; Proc. ICOSMFE V, Vol. I, p.213.

Leonards, G. A. and Ramiah, B. K. (1959). "Time Effects in the Consolidation of Clay," Special Technical Publication No.254, ASTM, 1959, p.116.

Leonards, G. A. and Altschaeffl, A. G. (1964). "Compressibility of clay"; ASCE Soil Mech. and Found. Div., September, 1964.

Lo, K. Y. (1961). "Secondary compression of clay"; ASCE Soil Mech. and Found. Div., August 1961, p.61.

--------. (1961). "Stress-strain relationship and pore water pressure characteristics of a normally consolidated clay"; Proc. ICOSMFE V, Vol. I, p.219.

Lo, M. B. (1964). "A preliminary report on consolidation of peat with respect to layer consolidation, pore water pressure and permeability"; McMaster University, Hamilton, Ontario.

McNabb, A. (1960). "A mathematical treatment of one dimensional soil consolidation"; Quart. Appl. Maths., 17:4.

Radforth, N. W. (1952). "Suggested classification of muskeg for the engineer"; The Engineering Journal, Vol. 35, November 1952, p.1194.

Schiffman, R. L. (1958). "Consolidation of soil under time dependent loading and varying permeability"; Proc. Highway Res. Board, Vol. 37.

Schiffman, R. L., Ladd, C. C. and Chen, T. F. (1964). "The secondary consolidation of clay"; Prepring of a paper prepared for Int. Union of Theoretical and Applied Mechanics Symposium on Rheology and Soil Mechanics, Rensselaer Poly. Inst., New York.

Schiffman, R. L. and Gibson, R. E. (1963). "Consolidation of non-homogeneous clay layers"; Proc. ASCE,' 90:SM5:1-30.

Schroeder, J. and Wilson, N. E. (1962). "The analysis of secondary consolidation of peat"; Proc. 8th Muskeg Research Conf., N.R.C., T.M. No.74, p.130.

Skempton, A. W. and Bjerrum, L. (1957). "A contribution to the settlement analysis of foundations on clay"; Geotechnique, Vol. VII, No. 4, pp.168-178.

Tan, T. K. (1957). "One-dimensional problems of consolidation and secondary time effects"; Inst. of Civil Eng. and Archi., Academia Sinica, China.

----------. (1957). "Two-dimensional problems of settlements of clay layers due to consolidation and secondary time effects"; Inst. of Civil Eng. and Archi., Academia Sinica, China.

----------. (1957). "Three-dimensional theory on the consolidation and flow of clay layers"; Inst. of Civil Eng. and Archi., Academia Sinica, China.

----------. (1957). "Structural mechanism of clays"; Inst. of Civil Eng. and Archi., Academia Sinica, China.

Taylor, D. W. (1942). "Research on consolidation of clays"; Publ. Serial 82, Dept. of Civil and Sanitary Eng., M.I.T.

Taylor, D. W. and Merchant, W. (1940). "A theory of clay consolidation accounting for secondary compressions"; J. Math. Phys., 19:3:167-185.

Terzaghi, K. (1925). "Erdbaumechanik auf bodenphysikalischer Grundlage"; Deuticke, Vienna.

----------. (1943). "Theoretical soil mechanics"; Wiley, New York.

Wahls, H. J. (1962). "Analysis of primary and secondary consolidation"; ASCE Soil Mech. and Found. Div., December 1962, p.207.

APPENDIX A

TABLES OF EXPERIMENTAL DATA

TABLE I

EXPERIMENTAL DATA

H = 2.946"

Temp. = 38.2°C

P_o = 2.60 psi

ΔP_o = 9.70 psi

P_f = 12.30 psi

e_o = 7.450 (average)

e_f = 4.580 (average)

Elapsed Time t (min.)	Total Pres. at the bottom P_B (psi)	#1 Pore W. Pres. u (psi)	#2 Pore W. Pres. u (psi)	#3 Pore W. Pres. u (psi)	#4 Pore W. Pres. u (psi)	#4 % of Max. Pore W.P. U (%)	Settle-ments s (ins.)	Sample Height $L(z_o,t)$ (ins.)	Degree of Primary Con-solidation S (%)
0							0.000	2.947	0
1	9.20	8.65	9.10	9.20	9.20	100	0.037	2.910	4.46
2	9.20	8.50	9.06	9.19	9.19	99.89	0.046	2.901	5.55
4	9.20	8.28	9.00	9.15	9.15	99.46	0.058	2.889	6.99
8	9.20	7.90	8.90	9.05	9.05	98.37	0.084	2.863	10.13
15	9.03	7.25	8.76	8.90	8.91	96.85	0.108	2.839	13.03
30	8.96	6.04	8.65	8.85	8.86	96.30	0.149	2.798	17.97
47	8.90	5.16	8.43	8.73	8.75	95.11	0.190	2.757	22.91
77	8.82	4.02	8.06	8.43	8.55	92.93	0.239	2.708	28.83
100	8.82	3.30	7.72	8.25	8.35	90.76	0.271	2.676	32.69
150	8.90	1.75	7.05	7.75	8.08	87.83	0.332	2.675	40.04
220	9.02	1.05	6.28	7.15	7.46	81.09	0.400	2.615	48.25
340	9.32	0.35	5.14	6.04	6.44	70.00	0.495	2.542	59.71
470	9.76	0.04	4.02	4.83	5.16	56.09	0.571	2.376	68.88
590	10.20	0	3.02	3.82	4.12	44.78	0.628	2.319	75.75
1060	11.25	0	1.01	1.41	1.54	16.74	0.743	2.204	89.63

TABLE I (Continued)

Elapsed Time t (min.)	Total Pres. at the bottom P_B (psi)	#1 Pore W. Pres. u (psi)	#2 Pore W. Pres. u (psi)	#3 Pore W. Pres. u (psi)	#4 Pore W. Pres. u (psi)	#4 % of Max. Pore W.P. U (%)	Settle-ments s (ins.)	Sample Height $L(z_o,t)$ (ins.)	Degree of Primary Con-solidation S (%)
1150	11.25	0	0.85	1.17	1.29	14.02	0.755	2.192	91.07
1665	11.70	0	0.22	0.42	0.44	4.78	0.792	2.155	95.54
1810	11.75	0	0.15	0.32	0.39	4.24	0.800	2.147	96.50
2545	11.78	0	0.05	0.10	0.10	1.09	0.819	2.127	98.79
4390	12.00	0	0	0	0	0	0.840	2.106	101.32
5765	12.00	0	0	0	0	0	0.848	2.098	102.29
7225	12.00	0	0	0	0	0	0.855	2.092	103.13
10585	12.00	0	0	0	0	0	0.860	2.087	103.74
14985	12.00	0	0	0	0	0	0.865	2.082	104.34
21745	12.00	0	0	0	0	0	0.870	2.077	104.95
27505	12.00	0	0	0	0	0	0.874	2.073	105.42

t_{100} = Elapsed time at the end of primary consolidation = 3500 (min.)

t_{50} = Elapsed time at 50% degree of consolidation = 540 (min.)

s_{100} = Settlement at the end of primary consolidation = 0.829"

TABLE II

DATA AT THE POSITIONS OF MARKERS

Marker A

Elapsed Time t (min.)	Height Above Base L' (ins.)	Change of Height $\Delta L'$ (ins.)	Time Interval Δt (min.)	Hydraulic Gradient i (psi/in.)	Pore Pres. u (psi)	Total Pres. at the bottom P_B (psi)	(1) $P_B-9.70$	(2) $\frac{L'}{L}(z_o,t)$	(3) (1)x(2)	Total Pres. Increment $\Delta P_T=P_B-(3)$ (psi)
8	2.5441	0.0125	7	4.34	7.34	9.20	-0.58	0.890	-0.516	9.636
15	2.5316	0.0375	15	7.20	6.32	9.03	-0.71	0.891	-0.632	9.622
30	2.4941	0.0364	17	8.60	5.18	8.96	-0.77	0.893	-0.687	9.617
47	2.4577	0.0740	53	8.20	4.56	8.90	-0.84	0.891	-0.748	9.608
100	2.3837	0.1231	120	8.56	3.22	8.82	-0.78	0.889	-0.693	9.613
220	2.2606	0.0990	120	6.56	1.88	9.02	-0.53	0.885	-0.469	9.639
340	2.1616	0.0750	130	5.46	1.58	9.32	-0.16	0.880	-0.140	9.681
470	2.0866	0.0525	120	4.84	1.53	9.76	+0.28	0.878	+0.245	9.634
590	2.0341	0.1060	470	3.60	1.12	10.20	+1.02	0.876	+0.893	9.826
1060	1.9281	0.0665	750	1.28	0.37	11.25	+1.80	0.871	+1.567	9.932
1810	1.8616	0.0275	735	0.32	0.08	11.75	+2.06	0.865	+1.781	9.978
2545	1.8341	0.0215	3220	0.09	0.02	11.78	+2.19	0.865	+1.894	9.996
5765	1.8126	0.0025	1460	0	0	12.00	+2.30	0.868	+1.996	10.003
7225	1.8101			0	0	12.00				

(*Total pressures are assumed to vary linearily through the depth)

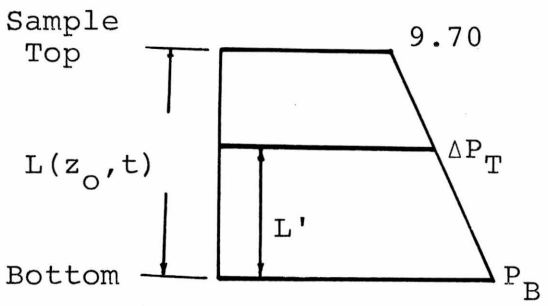

TABLE II (Continued)

Marker B

Elapsed Time t (min.)	Height Above Base L' (ins.)	Change of Height $\Delta L'$ (ins.)	Time Interval Δt (min.)	Hydraulic Gradient i (psi/in.)	Pore Pres. u (psi)	Total Pres. at the bottom P_B (psi)	(1) $P_B-9.70$	(2) $\frac{L'}{L}(z_o,t)$	(3) (1)x(2)	Total Pres. Increment $\Delta P_T=P_B-(3)$ (psi)
8	2.0133	0.0020	7	1.14	8.38	9.20	-0.58	0.707	-0.410	9.530
15	2.0113	0.0180	15	1.46	8.16	9.03	-0.71	0.711	-0.504	9.495
30	1.9933	0.0180	17	2.87	9.56	8.96	-0.77	0.716	-0.551	9.481
47	1.9753	0.0495	53	3.56	7.00	8.90	-0.84	0.718	-0.603	9.463
100	1.9258	0.1100	120	4.11	6.05	8.82	-0.78	0.717	-0.559	9.479
220	1.8158	0.0850	120	4.92	4.52	9.02	-0.53	0.710	-0.376	9.546
340	1.7308	0.0735	130	4.49	3.82	9.32	-0.16	0.702	-0.112	9.652
470	1.6573	0.0515	120	3.28	3.18	9.76	+0.28	0.695	+0.194	9.785
590	1.6058	0.1000	470	2.70	2.42	10.20	+1.02	0.688	+0.701	10.018
1060	1.5058	0.0565	750	1.13	0.86	11.25	+1.80	0.679	+1.222	10.277
1810	1.4493	0.0200	735	0.26	0.20	11.75	+2.06	0.674	+1.388	10.371
2545	1.4293	0.0217	3220	0.08	0.06	11.78	+2.19	0.673	+1.473	10.416
5765	1.4076	0.0043	1460	0	0	12.00	+2.30	0.674	+1.550	10.449
7225	1.4033			0	0	12.00				

TABLE II (Continued)

Marker C

Elapsed Time t (min.)	Height Above Base L' (ins.)	Change of Height $\Delta L'$ (ins.)	Time Interval Δt (min.)	Hydraulic Gradient i (psi/in.)	Pore Pres. u (psi)	Total Pres. at the bottom P_B (psi)	(1) $P_B-9.70$	(2) $\frac{L'}{L}(z_o,t)$	(3) (1)x(2)	Total Pres. Increment $\Delta P_T=P_B-(3)$ (psi)
8	1.7171	0	7	0.86	8.62	9.20	-0.58	0.602	-0.349	9.469
15	1.7171	0.0050	15	0.91	8.49	9.03	-0.71	0.608	-0.431	9.421
30	1.7121	0.0070	17	2.10	8.13	8.96	-0.77	0.616	-0.474	9.404
47	1.7051	0.0380	53	2.49	7.80	8.90	-0.84	0.621	-0.521	9.381
100	1.6671	0.0875	120	3.05	7.00	8.82	-0.78	0.622	-0.485	9.405
220	1.5796	0.0710	120	3.75	5.60	9.02	-0.53	0.618	-0.327	9.497
340	1.5086	0.0630	130	3.36	4.71	9.32	-0.16	0.612	-0.097	9.637
470	1.4456	0.0435	120	2.55	3.84	9.76	+0.28	0.607	+0.168	9.810
590	1.4021	0.0880	470	2.28	2.97	10.20	+1.02	0.601	+0.613	10.107
1060	1.3141	0.0520	750	0.94	1.07	11.25	+1.80	0.592	+1.065	10.434
1810	1.2621	0.0190	735	0.20	0.24	11.75	+2.06	0.587	+1.209	10.550
2545	1.2431	0.0210	3220	0.07	0.07	11.78	+2.19	0.585	+1.281	10.608
5765	1.2221	0.0025	1460	0	0	12.00	+2.30	0.585	+1.345	10.654
7225	1.2196			0	0	12.00				

TABLE II (Continued)

Marker D

Elapsed Time t (min.)	Height Above Base L' (ins.)	Change of Height $\Delta L'$ (ins.)	Time Interval Δt (min.)	Hydraulic Gradient i (psi/in.)	Pore Pres. u (psi)	Total Pres. at the bottom P_B (psi)	(1) $P_B-9.70$	(2) $\frac{L'}{L}(z_o,t)$	(3) (1)x(2)	Total Pres. Increment $\Delta P_T=P_B-(3)$ (psi)
8	1.4085	0	7	0.57	8.84	9.20	-0.58	0.495	-0.287	9.407
15	1.4085	0.0025	15	0.62	8.72	9.03	-0.71	0.499	-0.354	9.344
30	1.4060	0.0050	17	0.81	8.59	8.96	-0.77	0.506	-0.389	9.319
47	1.4010	0.0290	53	1.33	8.40	8.90	-0.84	0.510	-0.428	9.288
100	1.3720	0.0735	120	2.00	7.72	8.82	-0.78	0.511	-0.398	9.318
220	1.2985	0.0600	120	2.57	6.46	9.02	-0.53	0.508	-0.269	9.439
340	1.2385	0.0525	130	2.18	5.42	9.32	-0.16	0.502	-0.080	9.620
470	1.1860	0.0351	120	1.73	4.38	9.76	+0.28	0.498	+0.139	9.840
590	1.1509	0.0704	470	1.67	3.46	10.20	+1.02	0.493	+0.502	10.217
1060	1.0805	0.0410	750	0.76	1.26	11.25	+1.80	0.487	+0.876	10.623
1810	1.0395	0.0135	735	0.18	0.38	11.75	+2.06	0.484	+0.997	10.763
2545	1.0260	0.0148	3220	0	0.08	11.78	+2.19	0.483	+1.057	10.832
5765	1.0112	0.0016	1460	0	0	12.00	+2.30	0.484	+1.113	10.886
7225	1.0096			0	0	12.00				

TABLE III

CALCULATIONS IN DIFFERENT ZONES

Zone AB

Thickness of solid particles, z_{AB}= 0.0676"

Elapsed Time from t_1 to t_2 (min.)		Time Interval $\Delta t=t_2-t_1$ (min.)	Change in Thickness $\Delta L'$ (ins.)	Change in Hydraulic Gradient $\Delta i=i_A-i_B$ (psi/in.)	Average Permeability $k=\frac{L'}{\Delta t x \Delta i x 10.9}$ (cm./min.)	Change in Void Ratio Δe	Void Ratio e	Average Pore W. Pres. u (psi)	Average Total Pres. Increment ΔP_T (psi)
0	8						6.273		
8	15	7	0.0105	4.470	$3.08x10^{-5}$	0.155	6.118	7.55	9.583
15	30	15	0.0195	5.694	$2.09x10^{-5}$	0.289	5.829	6.81	9.558
30	47	17	0.0184	5.185	$1.91x10^{-5}$	0.273	5.556	6.08	9.549
47	100	53	0.0245	4.545	$9.33x10^{-6}$	0.363	5.193	5.21	9.535
100	220	120	0.0131	3.045	$3.29x10^{-6}$	0.195	4.998	3.92	9.546
220	340	120	0.0140	1.305	$8.21x10^{-6}$	0.207	4.791	2.95	9.592
340	470	130	0.0015	1.265	$8.36x10^{-7}$	0.022	4.769	2.53	9.666
470	590	120	0.0010	1.230	$6.21x10^{-7}$	0.015	4.754	2.06	9.759
590	1060	470	0.0060	0.525	$2.23x10^{-6}$	0.009	4.745	1.19	9.922
1060	1810	750	0.0100	0.105	$1.16x10^{-5}$	0.148	4.597	0.38	10.104
1810	2545	735	0.0075	0.035	$2.67x10^{-5}$	0.110	4.487	0.04	10.174
2545	5765	3220	0			0	4.487		10.206
5765	7225	1460	0			0	4.487		10.226
						Σ=1.786			

TABLE III (Continued)

Zone BC

Thickness of solid particles, z_{BC}= 0.0377"

Elapsed Time from t_1 to t_2 (min.)		Time Interval $\Delta t=t_2-t_1$ (min.)	Change in Thickness $\Delta L'$ (ins.)	Change in Hydraulic Gradient $\Delta i=i_B-i_C$ (psi/in.)	Average Permeability $k=\frac{L'}{\Delta t x \Delta i x 10.9}$ (cm./min.)	Change in Void Ratio Δe	Void Ratio e	Average Pore W. Pres. u (psi)	Average Total Pres. Increment ΔP_T (psi)
							7.471		
8	15	7	0.0020	0.415	$6.31x10^{-5}$	0.053	7.418	8.41	9.499
15	30	15	0.0130	0.660	$1.20x10^{-4}$	0.345	7.073	8.09	9.458
30	47	17	0.0110	0.920	$6.46x10^{-5}$	0.292	6.781	7.62	9.442
47	100	53	0.0115	1.065	$1.87x10^{-5}$	0.305	6.476	6.96	9.422
100	220	120	0.0225	1.115	$1.54x10^{-5}$	0.596	5.880	5.79	9.442
220	340	120	0.0140	1.150	$9.60x10^{-6}$	0.372	5.508	4.66	9.521
340	470	130	0.0105	0.930	$8.27x10^{-6}$	0.279	5.229	3.89	9.644
470	590	120	0.0080	0.575	$1.06x10^{-5}$	0.212	5.017	3.10	9.797
590	1060	470	0.0120	0.305	$7.68x10^{-6}$	0.318	4.699	1.83	10.062
1060	1810	750	0.0045	0.125	$4.40x10^{-6}$	0.119	4.580	0.59	10.355
1810	2545	735	0.0010	0.035	$3.56x10^{-6}$	0.027	4.553	0.14	10.460
2545	5765	3220	0.0007	0		0.019	4.534	0.003	10.512
5765	7225	1465	0.0018	0		0.047	4.487	0	10.551
						Σ=2.984			

TABLE III (Continued)

Zone CD

Thickness of solid particles, z_{CD}= 0.0392"

Elapsed Time from t_1 to t_2 (min.)		Time Interval $\Delta t=t_2-t_1$ (min.)	Change in Thickness $\Delta L'$ (ins.)	Change in Hydraulic Gradient $\Delta i=i_C-i_D$ (psi/in.)	Average Permeability $k=\frac{L'}{\Delta t x \Delta i x 10.9}$ (cm./min.)	Change in Void Ratio Δe	Void Ratio e	Average Pore W. Pres. u (psi)	Average Total Pres. Increment ΔP_T (psi)
							7.009		
8	15	7	0	0.290		0	7.009	9.00	9.438
15	30	15	0.0025	0.790	$1.94x10^{-5}$	0.064	6.945	8.48	9.382
30	47	17	0.0020	1.225	$8.81x10^{-6}$	0.051	6.894	8.23	9.361
47	100	53	0.0090	1.105	$1.41x10^{-5}$	0.229	6.665	7.73	9.334
100	220	120	0.0140	1.115	$9.60x10^{-6}$	0.357	6.308	6.69	9.361
220	340	120	0.0110	1.180	$7.12x10^{-6}$	0.281	6.027	5.55	9.444
340	470	130	0.0105	1.000	$7.41x10^{-6}$	0.268	5.759	4.59	9.628
470	590	120	0.0084	0.715	$9.80x10^{-6}$	0.214	5.545	3.66	9.825
590	1060	470	0.0176	0.395	$8.70x10^{-6}$	0.449	5.096	2.19	10.162
1060	1810	750	0.0110	0.100	$1.35x10^{-5}$	0.281	4.815	0.74	10.528
1810	2545	735	0.0055	0.045	$1.53x10^{-5}$	0.140	4.675	0.19	10.656
2545	5765	3220	0.0062	0.035	$5.05x10^{-6}$	0.164	4.511	0.04	10.720
5765	7225	1460	0.0009	0		0.024	4.487		10.770
						Σ=2.522			

TABLE IV

RELATIONSHIP BETWEEN VOID RATIO (e), PERMEABILITY (k)
AND EFFECTIVE PRESSURE (P')

Zone AB

Elapsed Time From t_1 to t_2 (min.)		Average Void ratio e	Permeability k (cm./min.)	$\frac{k}{1+e}$ (cm./min.)	Average Pore Pres. u (psi)	Total Pres. $P_T=2.60+\Delta P_T$ (psi)	Effective Pressure P' (psi)
8	15	6.196	3.08×10^{-5}	4.280×10^{-6}	7.550	12.183	4.633
15	30	5.973	2.09×10^{-5}	2.997×10^{-6}	6.810	12.158	5.348
30	47	5.693	1.91×10^{-5}	2.854×10^{-6}	6.080	12.149	6.069
47	100	5.375	9.33×10^{-6}	1.265×10^{-6}	5.210	12.135	6.925
100	220	5.096	3.29×10^{-6}	5.397×10^{-7}	3.920	12.146	8.226
220	340	4.896	8.21×10^{-6}	1.392×10^{-6}	2.950	12.192	9.242
340	470	4.781	8.36×10^{-7}	1.446×10^{-7}	2.530	12.266	9.736
470	590	4.762	6.21×10^{-7}	1.078×10^{-7}	2.060	12.359	10.299
590	1060	4.750	2.23×10^{-6}	3.878×10^{-7}	1.190	12.522	11.332
1060	1810	4.672	1.16×10^{-5}	2.045×10^{-6}	0.380	12.704	12.324
1810	2545	4.542	2.67×10^{-5}	4.817×10^{-6}	0.040	12.774	12.734
2545	5765	4.487			0	12.806	12.806
5765	7225	4.487			0	12.826	12.826

TABLE IV (Continued)

Zone BC

Elapsed Time From t_1 to t_2 (min.)		Average Void Ratio e	Permeability k (cm./min.)	$\frac{k}{1+e}$ (cm./min.)	Average Pore Pres. u (psi)	Total Pres. $P_T-2.60+\Delta P_T$ (psi)	Effective Pressure P' (psi)
8	15	7.444	6.31×10^{-5}	7.473×10^{-6}	8.410	12.099	3.689
15	30	7.246	1.20×10^{-4}	1.455×10^{-5}	8.090	12.058	3.968
30	47	6.927	6.46×10^{-5}	8.149×10^{-6}	7.620	12.042	4.422
47	100	6.629	1.87×10^{-5}	2.451×10^{-6}	6.960	12.022	5.062
100	220	6.178	1.54×10^{-5}	2.145×10^{-6}	5.790	12.042	6.252
220	340	5.694	9.60×10^{-6}	1.434×10^{-6}	4.660	12.121	7.461
340	470	5.369	8.27×10^{-6}	1.298×10^{-6}	3.890	12.244	8.354
470	590	5.124	1.06×10^{-5}	1.731×10^{-6}	3.100	12.397	9.297
590	1060	4.858	7.68×10^{-6}	1.311×10^{-6}	1.830	12.662	10.832
1060	1810	4.639	4.40×10^{-6}	7.803×10^{-7}	0.590	12.955	12.365
1810	2545	4.566	3.56×10^{-6}	6.396×10^{-7}	0.140	13.060	12.920
2545	5765	4.544			0.030	13.112	13.082
5765	7225	4.511			0	13.151	13.151

TABLE IV (Continued)

Zone CD

Elapsed Time From t_1 to t_2 (min.)		Average Void Ratio e	Permeability k (cm./min.)	$\frac{k}{1+e}$ (cm./min.)	Average Pore Pres. u (psi)	Total Pres. $P_T=2.60+\Delta P_T$ (psi)	Effective Pressure P' (psi)
8	15	7.009			9.000	12.038	3.038
15	30	6.977	1.94×10^{-5}	$2.432.10^{-6}$	8.480	11.982	3.502
30	47	6.920	8.81×10^{-6}	1.112×10^{-6}	8.230	11.961	3.731
47	100	6.780	1.41×10^{-5}	1.812×10^{-6}	7.730	11.934	4.204
100	220	6.486	9.60×10^{-6}	1.282×10^{-6}	6.690	11.961	5.271
220	340	6.167	7.12×10^{-6}	9.934×10^{-7}	5.550	12.044	6.494
340	470	5.893	7.41×10^{-6}	1.075×10^{-6}	4.590	12.228	7.638
470	590	5.652	9.80×10^{-6}	1.473×10^{-6}	3.660	12.425	8.765
590	1060	5.320	8.70×10^{-6}	1.376×10^{-6}	2.190	12.762	10.572
1060	1810	4.955	1.35×10^{-5}	2.267×10^{-6}	0.740	13.128	12.388
1810	2545	4.745	1.53×10^{-5}	2.663×10^{-6}	0.190	13.256	13.066
2545	5765	4.593	5.05×10^{-6}	9.029×10^{-7}	0.040	13.320	13.280
5765	7225	4.499			0	13.370	13.370

TABLE V

DATA FOR DETERMINATION OF

THE FLOW-LOADING PARAMETER (θ)

Zone AB

$(P'_1)=4.633$(psi) $\quad \frac{k_1}{1+e_1} = 4.280\text{x}10^{-6}$ cm./min.

P'/P'_1	$\frac{k}{1+e} \Big/ \frac{k_1}{1+e_1}$
1.000	$1.50\text{x}10^{0}$
1.154	$7.00\text{x}10^{-1}$
1.309	$6.67\text{x}10^{-1}$
1.495	$2.95\text{x}10^{-1}$
1.776	$1.26\text{x}10^{-1}$
1.990	$3.25\text{x}10^{-1}$
2.101	$3.38\text{x}10^{-2}$
2.223	$2.52\text{x}10^{-2}$
2.450	$9.06\text{x}10^{-2}$
2.660	$4.78\text{x}10^{-1}$
2.748	$1.12\text{x}10^{0}$

Zone BC

$P'_1 = 3.689$(psi) $\quad \frac{k_1}{1+e_1} = 7.473\text{x}10^{-6}$ cm./min.

P'/P'_1	$\frac{k}{1+e} \quad \frac{k_1}{1+e_1}$
1.000	$1.00\text{x}10^{0}$
1.075	$1.95\text{x}10^{0}$
1.198	$1.09\text{x}10^{0}$
1.372	$3.28\text{x}10^{-1}$
1.695	$2.87\text{x}10^{-1}$
2.022	$1.92\text{x}10^{-1}$
2.265	$1.74\text{x}10^{-1}$
2.520	$2.32\text{x}10^{-1}$
2.936	$1.75\text{x}10^{-1}$
3.351	$1.04\text{x}10^{-1}$
3.502	$8.56\text{x}10^{-2}$

TABLE V (Continued)

Zone CD

$(P_1')=3.038$(psi) $\quad \frac{k_1}{1+e_1} = 2.432\text{x}10^{-6}$ cm./min.

P'/P_1'	$\frac{k}{1+e} \Big/ \frac{k_1}{1+e_1}$
1.000	$1.00\text{x}10^{0}$
1.152	$4.57\text{x}10^{-1}$
1.228	$7.45.10^{-1}$
1.384	$5.27\text{x}10^{-1}$
1.735	$4.08\text{x}10^{-1}$
2.137	$4.42\text{x}10^{-1}$
2.514	$6.06\text{x}10^{-1}$
2.885	$5.66\text{x}10^{-1}$
3.480	$9.32\text{x}10^{-1}$
4.078	$1.09\text{x}10^{0}$
4.300	$3.71\text{x}10^{-1}$

TABLE VI

GENERAL RELATIONSHIP BETWEEN VOID RATIO (e), PERMEABILITY (k)

AND EFFECTIVE PRESSURE (P') OF THE PEAT SAMPLE

Effective Pressure P' (psi)	Void Ratio e	Permeability k (cm./min.)	$\frac{k}{1+e}$ (cm./min.)	$\frac{k}{1+e} / \frac{k_o}{1+e_o}$	P'/P'_o
2.60	7.65	1.00×10^{-4}	1.16×10^{-5}	1	1
3.00	7.40	7.80×10^{-5}	9.29×10^{-6}	7.92×10^{-1}	1.15
4.00	6.82	4.11×10^{-5}	5.24×10^{-6}	4.83×10^{-1}	1.54
5.00	6.40	2.52×10^{-5}	3.38×10^{-6}	3.14×10^{-1}	1.92
6.00	6.02	1.60×10^{-5}	2.28×10^{-6}	2.24×10^{-1}	2.31
7.00	5.75	1.17×10^{-5}	1.73×10^{-6}	1.75×10^{-1}	2.69
8.00	5.48	8.60×10^{-6}	1.33×10^{-6}	1.25×10^{-1}	3.08
9.00	5.25	6.61×10^{-6}	1.06×10^{-6}	1.08×10^{-1}	3.46
10.00	5.00	5.00×10^{-6}	8.33×10^{-7}	9.16×10^{-2}	3.85
11.00	4.73	3.60×10^{-6}	6.28×10^{-7}	7.66×10^{-2}	4.23
12.00	4.65	3.31×10^{-6}	5.84×10^{-7}	6.59×10^{-2}	4.62

TABLE VII

COMPARISONS OF EXPERIMENTAL DATA TO PREVIOUS THEORIES

1) Pore Pressure Dissipation at the Bottom. (χ=1)

Curves were fitted at U=50% (U=Percentage of max. pore pressure).

T_{50}^{U}= Time factor at U=50%

T_{50}^{U}= 1.300 ——— The extended theory (for Δ=3.73, θ=61°)

T_{50}^{U}= 0.380 ——— The Terzaghi theory

T_{50}^{U}= 0.560 ——— The Davis and Raymond theory

t_{50}^{U}= 540 (min.) = Elapsed time from U=100% to U=50%

t_{100}^{U}= 3500 (min.) = Elapsed time from U=100% to U=0%

TABLE VII (Continued)

Pore Pres. u (psi)	Percentage of Max. P. Pres. U (%)	Elapsed Time t (min.)	The Extended Theory T	The Terzaghi Theory T	The Davis and Raymond Theory T
9.20	100	1	0.002	0.001	0.001
9.19	99.89	2	0.005	0.002	0.002
9.15	99.46	4	0.010	0.003	0.004
9.05	98.37	8	0.020	0.006	0.008
8.92	96.96	15	0.036	0.011	0.016
8.86	96.30	30	0.072	0.021	0.031
8.75	95.11	47	0.113	0.033	0.049
8.55	92.93	77	0.186	0.054	0.080
8.36	90.87	100	0.241	0.070	0.104
8.13	88.37	150	0.362	0.105	0.155
7.56	82.17	220	0.530	0.155	0.228
6.56	71.30	340	0.819	0.239	0.352
5.23	56.85	470	1.130	0.331	0.488
4.18	45.43	590	1.420	0.415	0.612
1.56	16.96	1060	2.550	0.745	1.100
0.47	5.11	1665	4.000	1.170	1.727
0.39	4.24	1810	4.360	1.275	1.877
0.10	1.09	2545	6.140	1.791	2.639
0	0	4390			

TABLE VII (Continued)

2) Degree of Consolidation.

Curves fitted at S=50% (S=Degree of consolidation).

T_{50}^{S} = Time factor at S=50%

T_{50}^{S} = 0.420 ——— The extended theory (for Δ=3.73, θ=61°)

T_{50}^{S} = 0.195 ——— The Terzaghi theory; the Davis and Raymond theory

t_{50}^{S} = 240 (min.) = Elapsed time from S=0% to S=50%

t_{100}^{S} = 3500 (min.) = Elapsed time from S=0% to S=100%

s_{100} = 0.829" (Primary Compression)

TABLE VII (Continued)

Settlement s (ins.)	Degree of Consolidation S (%)	Elapsed Time t (min.)	The Extended Theory T	The Terzaghi Theory; the Davis and Raymond Theory T
0.037	4.46	1	0.002	0.001
0.046	5.55	2	0.004	0.002
0.058	6.99	4	0.007	0.003
0.084	10.13	8	0.014	0.006
0.108	13.03	15	0.026	0.012
0.149	17.97	30	0.053	0.024
0.190	22.91	47	0.082	0.038
0.239	28.83	77	0.135	0.063
0.271	32.69	100	0.175	0.081
0.332	40.04	150	0.263	0.122
0.400	48.25	220	0.385	0.179
0.495	59.71	340	0.595	0.276
0.571	68.88	470	0.822	0.382
0.628	75.75	590	1.033	0.479
0.743	89.63	1060	1.855	0.861
0.755	91.07	1150	2.021	0.938
0.792	95.54	1665	2.914	1.353
0.800	96.50	1810	3.147	1.461
0.819	98.79	2545	4.54	2.068
0.840	101.32	4390	7.681	3.566

TABLE VIII

CALCULATIONS FOR THEORETICAL CURVES OF CONSOLIDATION AND DISSIPATION OF PORE PRESSURE AT SAMPLE BOTTOM

Δ = Load Increment Ratio

θ = The Flow-Loading Parameter

S = Degree of Consolidation

U = Percentage of Max. Pore Pressure

T = Time Factor

1) $\theta = 0^{\circ}$

T	Δ=0.25		Δ=0.5		Δ=1		Δ=2		Δ=4		Δ=8	
	S	U	S	U	S	U	S	U	S	U	S	U
0.001	5.6	100	5.6	100	6.2	100	6.6	100	7.1	100	8.1	100
0.002	6.9	100	7.0	100	7.4	100	8.2	100	9.3	100	11.0	100
0.004	8.6	100	8.9	100	9.6	100	11.1	100	12.7	100	15.5	100
0.008	11.4	100	12.0	100	13.0	100	15.0	100	17.8	100	21.7	100
0.010	12.8	100	13.5	100	14.4	100	16.3	100	20.0	100	24.3	100
0.020	17.2	100	18.2	100	20.2	100	22.5	100	28.0	100	34.2	100
0.040	24.3	100	25.7	99.8	28.2	99.8	32.5	99.7	39.1	99.6	48.3	99.3
0.080	34.3	97.0	36.5	96.7	40.0	96.2	46.9	95.7	55.5	93.0	68.2	84.4
0.100	39.0	94.3	40.7	94.0	44.9	93.1	52.0	91.0	61.2	86.0	75.9	70.4
0.200	54.2	75.6	57.4	73.7	63.1	69.6	72.0	60.0	85.0	44.0	96.3	14.3
0.400	74.4	43.7	78.4	39.5	84.6	31.9	92.0	20.2	98.2	5.5	100	0.2
0.700	89.6	18.0	90.9	17.1	96.0	9.0	99.1	2.5	100	0.1		
1.000	95.9	7.0	97.6	4.8	99.2	1.9	99.9	0.2				
1.500	99.2	1.8	99.6	0.8	100	0.1						
2.000	99.9	0.1	100	0.1								

TABLE VIII (Continued)

2) $\theta = 15^{\circ}$

T	Δ=0.25		Δ=0.5		Δ=1		Δ=2		Δ=4		Δ=8	
	S	U	S	U	S	U	S	U	S	U	S	U
0.001	5.5	100	5.6	100	5.6	100	6.2	100	6.6	100	7.1	100
0.002	6.8	100	6.9	100	7.1	100	7.6	100	8.3	100	9.7	100
0.004	8.5	100	8.7	100	9.1	100	9.8	100	11.0	100	13.1	100
0.008	11.2	100	11.6	100	12.3	100	13.5	100	15.5	100	18.0	100
0.010	12.4	100	13.0	100	13.7	100	15.5	100	17.2	100	20.0	100
0.020	17.3	100	17.9	100	19.0	100	21.0	100	24.0	100	27.5	100
0.040	24.1	100	25.0	99.9	26.8	99.9	29.5	99.8	33.8	99.3	39.2	99.1
0.080	33.8	97.6	35.3	97.4	37.7	97.2	41.6	97.1	48.0	96.8	56.0	95.1
0.100	37.7	94.9	39.3	94.6	42.2	94.2	47.0	93.6	54.0	91.4	62.4	90.0
0.200	53.1	76.8	55.5	75.8	59.4	74.3	65.0	70.1	75.0	61.0	85.1	50.0
0.400	73.1	45.6	76.1	43.4	80.5	39.1	86.9	31.2	93.5	19.0	98.0	6.0
0.700	88.6	20.0	90.9	17.2	94.2	12.8	97.5	7.5	99.4	2.0	100	0.1
1.000	95.3	8.1	96.6	6.6	98.4	3.9	99.6	1.9	100	0.1		
1.400	98.0	3.2	98.8	2.2	99.5	1.1	100	0.1				
2.000	99.7	0.4	99.9	0.2	100	0.0						
2.100	99.8	0.2	100	0.0								
2.200	100	0.1										

3) $\theta = 30^{\circ}$

T	Δ=0.25		Δ=0.5		Δ=1		Δ=2		Δ=4		Δ=8	
	S	U	S	U	S	U	S	U	S	U	S	U
0.001	5.5	100	5.5	100	5.6	100	5.6	100	6.2	100	6.4	100
0.002	6.8	100	6.8	100	6.9	100	7.1	100	7.4	100	7.9	100
0.004	8.3	100	8.5	100	8.7	100	9.0	100	9.6	100	10.7	100
0.008	11.0	100	11.2	100	11.6	100	12.2	100	13.5	100	14.4	100
0.010	12.1	100	12.5	100	12.8	100	13.3	100	14.6	100	16.0	100
0.020	16.8	100	17.2	100	17.8	100	18.7	100	20.0	100	22.0	100
0.040	23.5	100	24.1	99.8	25.0	99.9	26.4	99.9	28.4	99.9	30.7	99.9
0.080	33.1	96.4	33.9	97.5	35.2	97.7	37.2	98.0	40.0	98.0	44.0	97.8
0.100	36.9	95.1	37.7	95.2	39.4	95.4	42.0	96.3	44.5	96.2	49.0	96.0
0.200	51.9	77.6	53.3	78.1	55.4	78.6	58.8	79.1	63.0	79.0	69.0	78.5
0.400	71.8	47.6	73.4	47.3	76.0	46.9	79.6	45.5	84.2	42.0	90.0	36.0
0.800	90.5	16.3	91.6	15.5	93.4	14.2	95.6	11.3	97.8	7.3	99.1	4.0
1.300	97.3	5.0	97.8	4.2	98.6	3.2	99.2	1.8	99.7	0.7	100	
1.600	98.9	2.0	99.2	1.6	99.5	1.1	99.8	0.5	100	0.1		
2.000	99.6	0.8	99.7	0.4	99.9	0.3	100	0.1				
2.400	99.9	0.3	99.9	0.2	100	0.1						
2.500	100	0.2	100	0.1								

TABLE VIII (Continued)

4) $\theta = 45^{\circ}$

T	Δ=0.25		Δ=0.5		Δ=1		Δ=2		Δ=4		Δ=8	
	S	U	S	U	S	U	S	U	S	U	S	U
0.001	5.1	100	5.1	100	5.1	100	5.1	100	5.1	100	5.1	100
0.002	6.1	100	6.1	100	6.1	100	6.1	100	6.1	100	6.1	100
0.004	8.0	100	8.0	100	8.0	100	8.0	100	8.0	100	8.0	100
0.008	10.6	100	10.6	100	10.6	100	10.6	100	10.6	100	10.6	100
0.010	12.0	100	12.0	100	12.0	100	12.0	100	12.0	100	12.0	100
0.020	16.0	100	16.0	100	16.0	100	16.0	100	16.0	100	16.0	100
0.040	22.6	99.9	22.6	99.9	22.6	99.9	22.6	99.9	22.6	99.9	22.6	99.9
0.080	31.9	97.5	31.9	98.0	31.9	98.1	31.9	98.5	31.9	98.9	31.9	99.2
0.100	35.7	94.5	35.7	94.8	35.7	96.0	35.7	96.9	35.7	97.8	35.7	98.1
0.200	50.4	78.0	50.4	78.0	50.4	82.0	50.4	86.0	50.4	88.6	50.4	92.0
0.400	69.8	50.0	69.8	50.0	69.8	56.2	69.8	61.5	69.8	67.5	69.8	72.5
0.800	88.7	19.2	88.7	19.6	88.7	23.0	88.7	25.1	88.7	30.0	88.7	37.0
1.000	93.1	12.1	93.1	12.3	93.1	15.0	93.1	16.5	93.1	20.0	93.1	25.5
2.000	99.4	1.0	99.4	1.1	99.4	1.2	99.4	1.5	99.4	1.8	99.4	2.2
2.900	99.9	0.1	100	0.1	100	0.1	100	0.1	100	0.1	100	0.1

5) $\theta = 60^{\circ}$

T	Δ=0.25		Δ-0.5		Δ=1		Δ=2		Δ=4		Δ=8	
	S	U	S	U	S	U	S	U	S	U	S	U
0.001	5.5	100	5.4	100	5.4	100	5.3	100	5.3	100	5.3	100
0.002	6.6	100	6.5	100	6.3	100	6.2	100	6.0	100	5.9	100
0.004	8.0	100	7.8	100	7.5	100	7.2	100	6.9	100	6.6	100
0.008	10.4	100	10.1	100	9.6	100	9.1	100	8.5	100	8.0	100
0.010	11.4	100	10.9	100	10.6	100	9.8	100	9.1	100	8.6	100
0.020	15.5	100	14.9	100	14.2	100	13.2	100	12.0	100	11.0	100
0.040	21.8	99.9	20.9	99.9	19.7	99.9	18.1	99.9	16.5	99.9	14.9	100
0.080	30.5	98.0	29.3	98.2	27.5	98.8	25.2	99.1	22.8	99.5	20.4	99.7
0.100	34.0	96.0	32.6	96.6	30.7	97.5	28.1	98.3	25.4	99.0	22.7	99.4
0.200	48.0	81.6	46.0	84.4	43.1	88.1	39.5	91.9	35.6	95.0	31.7	97.3
0.400	66.5	54.8	64.0	60.4	60.2	68.2	55.3	77.2	49.8	85.4	44.4	91.5
0.800	86.0	24.0	83.4	30.0	79.5	39.5	74.0	52.7	67.3	67.3	60.4	79.7
1.000	90.8	16.0	88.7	21.0	85.0	29.8	79.8	43.3	73.0	59.4	65.8	74.1
2.00	98.9	2.0	98.2	3.4	96.7	7.0	93.7	15.2	88.8	30.1	82.3	49.5
3.00	99.9	0.1	99.8	0.2	99.3	1.6	98.0	3.4	94.9	15.0	90.0	32.0
3.50			100	0.1	99.6	0.9	98.8	3.0	96.8	9.5	92.6	24.1
4.40					99.9	0.1	99.6	1.1	98.4	5.1	95.4	16.5
6.00							100	0.2	99.5	1.6	97.9	7.7
8.4									100	0.1	99.4	2.1
12.50											100	0.2

TABLE VIII (Continued)

6) $\theta = 75^{\circ}$

T	Δ=0.25		Δ=0.5		Δ=1		Δ=2		Δ=4		Δ=8	
	S	U	S	U	S	U	S	U	S	U	S	U
0.001	5.4	100	5.3	100	5.2	100	5.2	100	5.1	100	5.1	100
0.002	6.3	100	6.0	100	5.8	100	5.5	100	5.4	100	5.3	100
0.004	7.4	100	7.0	100	6.5	100	6.0	100	5.7	100	5.5	100
0.008	9.4	100	8.6	100	7.7	100	6.9	100	6.4	100	6.0	100
0.010	10.2	100	9.4	100	8.3	100	7.3	100	6.6	100	6.2	100
0.020	13.7	100	12.3	100	10.5	100	8.9	100	7.8	100	7.1	100
0.040	19.1	100	16.8	100	14.0	100	11.5	100	9.6	100	8.3	100
0.080	26.8	98.4	23.2	99.0	19.1	99.4	15.2	99.6	12.2	99.8	10.5	99.9
0.100	29.8	96.9	25.9	98.0	21.2	98.8	16.7	99.3	13.4	99.6	11.2	99.8
0.200	41.9	86.0	36.3	90.4	29.5	94.1	22.9	96.8	17.8	98.4	14.5	99.2
0.400	58.5	64.8	50.7	74.6	41.2	84.3	31.6	91.4	24.3	95.6	19.3	97.8
0.800	77.6	37.2	68.5	51.6	56.3	68.6	43.4	82.4	33.1	90.7	26.0	96.1
1.000	90.5	16.8	74.5	43.1	61.6	62.3	47.8	78.6	36.3	88.9	28.3	94.4
2.000	95.8	7.2	89.8	18.4	77.8	40.2	62.1	64.2	47.5	81.1	36.8	90.4
4.00	99.9	0.1	98.0	4.0	91.0	18.1	76.2	46.1	59.5	70.5	46.3	84.9
7.00			99.9	0.1	97.5	5.2	86.4	29.5	69.7	59.3	54.6	78.9
10.00					99.1	1.9	91.3	19.9	75.3	51.9	59.6	74.6
16.00					99.9	0.2	96.2	9.2	82.6	40.4	66.2	68.2
20.00							97.8	5.6	85.7	34.8	69.3	64.6
40.00							99.9	0.2	93.7	17.5	78.8	52.0
50.00									95.7	12.5	81.5	47.1
90.00									99.0	2.5	88.2	33.0
160.00									99.9	0.1	94.1	18.0
250.00											96.1	10.1
400.00											98.0	4.8
600.00											99.2	1.1
1000.00											100	0.1

APPENDIX B

COMPUTER PROGRAM USED FOR ANALYSIS

TABLE IX

NOMENCLATURE USED FOR COMPUTER PROGRAM

Program Symbol	Meaning or Equivalent
A	Function
AAA	Function
ABC	Function
B	Function
BBB	Function
C(I,J)	C; $C=p^{1-n}$ (where $p = \frac{P'}{P'_o}$, the ratio of effective pres. to preconsolidated pres.)
CC	$\pi/180$
DEL	Δ, Load Increment Ratio
G	$(p_1)^{1-\tan\theta}$; $p_1 = \frac{P'_o+\Delta P'_o}{P'_o} = 1+\Delta$; θ=The Flow-Loading Parameter
I,J,K,L,J,N, IA,IB,IC,MM,	Counters
Out	Subroutine Function
P(I,J)	p (Ratio of effective pressure to pre-consolidated pres., $\frac{P'}{P'_o}$
PW(K)	$\frac{1}{1-\tan\theta}$
PROD	Function
Q	J, Counter

TABLE IX (Continued)

Program Symbol	Meaning or Equivalent
R	$\frac{\Delta T}{\Delta \chi^2}$
RR	R x 0.01
S	S, Degree of Consolidation
UC1	U (χ= 1/2), Percentage of Max. Pore Pressure at χ=1/2
UC2	U (χ=1), Percentage of Max. Pore Pressure at χ=1

TABLE X

COMPUTER PROGRAM FOR THE SOLUTION OF EQU.(5)

```
      A SOLUTION TO THE EXTENDED THEORY ON ONE DIMENSIONAL PRIMARY
      CONSOLIDATION OF SOILS
      THEORETICAL CURVES OF THE DEGREE OF CONSOLIDATION AND THE
      DISSIPATION OF MAXIMUM PORE WATER PRESSURE ARE OBTAINED FOR
      VARIOUS VALUES OF LOAD INCREMENT RATIO ( DEL ) AND THE
      FLOW-LOADING PARAMETER ( THE )

       COMMON C(12,400),T(400),ABC ,PW(5),K,N,DEL(6)
       COMMON S
      DIMENSION THE(6),THET(5)
      READ(5,1) DEL, THE
    1 FORMAT(6F10.3)
      WRITE(6,2) (DEL(N),N=1,6),(THE(K),K=1,5)
    2 FORMAT(1X,6F10.3/5X,5F12.3)
      CC=3.14159/180.0
      MM=0
      N=1
  606 K=1
  801 L=1
      AAA=DEL(N)
      ABC=ALOG10(1.0+AAA)*10.0
      BBB=THE(K)
      WRITE(6,222) AAA,BBB
  222 FORMAT(1H0,2X,5HDEL= ,F10.3,10X,5HTHE= ,F10.3)
      THET(K)=1.0-TAN(CC*THE(K))
      PW(K)=1.0/THET(K)
      G=(1.0+DEL(N))**THET(K)
      IF(G.LE.2.0) GO TO 100
      IF(G.LE.2.5) GO TO 200
      IF(G.LE.6.0) GO TO 300
      IF(G.LE.8.0) GO TO 400
      IF(G.LE.15.0) GO TO 500
      R=0.001
      GO TO 800
  100 R=0.1
      GO TO 800
  200 R=0.04
      GO TO 800
  300 R=0.03
      GO TO 800
  400 R=0.015
      GO TO 800
  500 R=0.01
  800 WRITE(6,444) R
  444 FORMAT(1H0,2X,3HR= ,F10.4)
      J=1
      DO 10 I=2,12
   10 C(I,J)=1.0
```

TABLE X (CONTINUED)

```
      I=1
      J=1
      Q=J
      T(J)=Q
      C(I,J)=(1.0+G)/2.0
      DO 11 J=2,400
      Q=J
      RR=R*0.01
      T(J)=(Q-1.0)*RR
   11 C(I,J)=G
   21 J=1
      DO 15 I=2,11
   15 C(I,J+1)=C(I,J)*(1.0+R*(C(I+1,J)+C(I-1,J)-2.0*C(I,J)))
      I=12
      C(I,J+1)=C(I-2,J+1)
      DO 35 J=2,399
      DO 40 I=2,11
      Z=C(I+1,J)+C(I-1,J)-2.0*C(I,J)
      A=C(I,J-1)+2.0*R*C(I,J)*Z
      B=C(I,J)*(1.0+R*Z)
      C(I,J+1)=(A+B)/2.0
   40 CONTINUE
      I=12
      C(I,J+1)=C(I-2,J+1)
   35 CONTINUE
      J=400
      IF(L.EQ.1) GO TO 101
      IF(L.EQ.2) GO TO 202
      IF(L.EQ.3) GO TO 303
      IF(L.LE.25) GO TO 404
      IF(L.EQ.(26+6*MM)) GO TO 505
      GO TO 808
  101  CALL OUT(1,10,1)
       CALL OUT(20,100,10)
       CALL OUT(150,400,50)
       IF( S.GT.0.999) GO TO 909
      GO TO 808
  202  CALL OUT(100,400,100)
       IF( S.GT.0.999) GO TO 909
      GO TO 808
  303  CALL OUT(200,400,200)
       IF( S.GT.0.999) GO TO 909
      GO TO 808
  404  CALL OUT(400,400,400)
       IF( S.GT.0.999) GO TO 909
      GO TO 808
  505  CALL OUT(400,400,400)
       IF( S.GT.0.999) GO TO 909
      MM=MM+1
  808 IF(L.EQ.150) GO TO 909
```

TABLE X (CONTINUED)

```
      L=L+1
      LL=(L-1)*399
      SS=LL
      J=1
      Q=J
      T(J)=(Q+SS-1.0)*RR
      DO 91 I=1,12
   91 C(I,J)=C(I,J+399)
      I=1
      DO 92 J=2,400
      Q=J
      T(J)=(Q+SS-1.0)*RR
   92 C(I,J)=G
      GO TO 21
  909 K=K+1
      IF(K.GT.1) GO TO 777
      GO TO 801
  777 N=N+1
      IF(N.GT.1) GO TO 333
      GO TO 606
  333 STOP
      END

       SUBROUTINE OUT(IA,IB,IC)
       COMMON C(12,400),T(400),ABC ,PW(5),K,N,DEL(6)
       COMMON S
      DIMENSION P(11)
      DO 10 J=IA,IB,IC
      PROD=1.0
      DO 11 M=1,11
      P(M)=C(M,J)**PW(K)
   11 PROD=PROD*P(M)
      S=ALOG10(PROD/SQRT(P(1)*P(11)))/ABC
      UC1  =(P(1)-P(6))/DEL(N)
      UC2=(P(1)-P(11))/DEL(N)
   10 WRITE(6,6)  S,T(J), UC1, UC2
    6 FORMAT(1H0,1X,4H S= ,F7.3,3X,3HT= ,F9.5,3X,9HUC(1/2)= ,F7.3,
     13X,7HUC(1)= ,F7.3)
       RETURN
       END
```

APPENDIX C

NOMENCLATURE

TABLE XI

NOMENCLATURE

A = Area of the loading piston.

A_1 = Volume to represent the total force acting at the sample bottom during the early stage of consolidation.

a = Compression index. Radius of the loading piston.

a' = $a/\text{Log}_e 10$.

B = $\sum_{N=o}^{N=\infty} \frac{2}{M} (\text{Sin } M\chi) e^{-M^2 T}$.

B_1 = Volume to represent the total force acting at the sample bottom at the end of consolidation.

C = $p^{(1-n)}$.

C_v = $\frac{k(1+e)}{a_{vc}\ \gamma_w}$, coefficient of consolidation by Terzaghi; where a_{vc} is coefficient of compressibility.

C_v' = $\frac{k_o(1+e_o)P'_o}{a'\ \gamma_w}$, coefficient of consolidation in the extended theory.

E = Modulus of elasticity of the soil.

e = Void ratio.

e_1 = Void ratio at the beginning time of measurement.

TABLE XI (Continued)

e_o = Initial void ratio.

f = Coefficient of friction between the soil sample and the cylinder wall.

G = Modulus of rigidity of the soil.

h = Pore water pressure head.

H = Initial depth of the soil stratum.

i = Hydraulic gradient = $\frac{\partial h}{\partial L}$.
Space dimension in numerical analysis.

j = Time dimension in numerical analysis

k = Permeability.

k_1 = Permeability at the beginning time of measurement.

k_o = Initial permeability.

L = L(z,o), Depth of layer at initial condition.

L(z,t) = Depth of layer at time t
= $\int_o^z \frac{1}{1+e(z,t)}\, dz$, z is the thickness of the solid particles in that layer.

M = (2N+1) $\pi/2$.

N = 0, 1, 2, 3 . . . ∞

n = tan θ.

P = Total pressure.

P_1 = Final total pressure = $P_o+\Delta P_o$.

TABLE XI (Continued)

P_o = Preconsolidated total pressure.

P' = Effective pressure.

P'_1 = Final effective pressure = P_1

= $P_o+\Delta P_o$

P'_o = Preconsolidated effective pressure.

ΔP_o = Total pressure increment.

p = Ratio of effective pressure to preconsolidated pressure.

= P'/P'_o

p_1 = Ratio of final effective pressure to preconsolidated pressure = P'_1/P'_o

= $\frac{P_o+\Delta P_o}{P_o} = 1 + \Delta$

R = $\frac{\Delta T}{\Delta \chi^2}$

S = Degree of consolidation.

T = Time factor = $\frac{C'_v t}{H^2}$

U = Percentage of max. pore water pressure.

U_r = Displacement of the soil particles in γ (radial) direction.

U_z = Displacement of the soil particles in z (verticle) direction.

u = Pore water pressure.

TABLE XI (Continued)

V	= Volume of the soil element.
v	= Vertical velocity of pore water flow. Poisson's ratio of the soil.
χ	= Depth ratio at initial condition $= \frac{L}{H} = \frac{L(z,o)}{L(z_o,o)}$
γ_w	= Unit weight of pore water.
Δ	= Load increment ratio.
θ	= The Flow-Loading Parameter.